




# The origins of neural spine elongation in iguanodontian dinosaurs and the osteology of a new sail-back styracosternan (Dinosauria, Ornithischia) from the Lower Cretaceous Wealden Group of England

by JEREMY A. F. LOCKWOOD<sup>1,2,\*</sup> , DAVID M. MARTILL<sup>2</sup>  and SUSANNAH C. R. MAIDMENT<sup>1</sup> 

<sup>1</sup>Fossil Reptiles, Amphibians and Birds Section, Natural History Museum, London SW7 5BD, UK; [jlockwood156@aol.com](mailto:jlockwood156@aol.com)

<sup>2</sup>School of the Environment and Life Sciences, University of Portsmouth, Portsmouth PO1 2DT, UK

\*Corresponding author

Typescript received 15 November 2024; accepted in revised form 8 July 2025

**Abstract:** The Wealden Group of southern England was deposited during the late Berriasian to early Aptian interval. It records a critical time in the development of iguanodontian dinosaur diversity, which increased from low levels during the Jurassic to higher levels in the Aptian and Albian. A new iguanodontian dinosaur, *Istiorachis macarthurae* gen. et sp. nov. from the Wessex Formation (Wealden Group) of the Isle of Wight, exhibits hyperelongation of the dorsal and caudal neural spines, suggesting that it possessed a possible sail structure. Ancestral state reconstruction for the relative height of dorsal neural spines in iguanodontians demonstrates that modest elongation began with Ankylopollexia in the Late Jurassic and elongation became established during the Berriasian stage of the Early Cretaceous, albeit with

widely disparate values. Hyperelongation of neural spines occurred more sporadically throughout the Cretaceous, being recorded most often in the Barremian and early Aptian. Possible explanations for neural spine elongation in Ankylopollexia include biomechanical advantage, perhaps related to greater mass and a locomotory shift towards quadrupedalism, and visual signalling driven either by sexual selection or species recognition, or both. The function of elongate neural spines was probably pluralistic and differed in different taxa. No single explanation fully supports the variation seen throughout the Cretaceous.

**Key words:** Iguanodontia, diversity, sexual signalling, Isle of Wight, ossified tendons, Barremian.

IGUANODONTIA was a highly successful clade of ornithischian dinosaurs, the earliest known example being the dryosaurid *Callovosaurus leedsii* Galton 1980 (Lydekker 1889a) from the Middle Jurassic Oxford Clay Formation of England (Ruiz-Omeñaca *et al.* 2007). By the end of the Cretaceous they dominated the dinosaur fauna of Laurasia as the duck-billed hadrosaurids, a group containing well-known taxa such as *Edmontosaurus regalis* Lambe 1917 and *Parasaurolophus walkeri* Parks 1922. Iguanodontian diversity was low in the Late Jurassic but increased throughout the Early Cretaceous (Weishampel *et al.* 2004; Barrett *et al.* 2009a). This period was marked by the appearance of striking variation in the relative height of dorsal neural spines in iguanodontians, with exceptionally tall examples being found in *Hypselospinus fittoni* Norman 2010 (Lydekker 1889b) from the Valanginian of England, *Morelladon beltrani* Gasulla *et al.* 2015 from the Barremian of Spain and *Ouranosaurus nigeriensis* Taquet 1976

from the Aptian of Niger (Bertoazzo *et al.* 2017). Neural spine elongation continued throughout the Cretaceous and is also found in hadrosaurids, for example *Hypacrosaurus altispinus* Brown 1913a from the Maastrichtian of Canada and *Barsboldia sicinskii* Maryńska & Osmólska 1981 from the Maastrichtian of Mongolia.

It is difficult to explain hyperelongation of neural spines purely in terms of their primary physiological function, which is to divide the right and left epaxial musculature (Romer 1956, ch. 6, pp. 218–297), and they are usually interpreted as providing support for a dorsal sail-like structure. Neural spines also provide a surface for the attachment of ligaments, tendons and muscles and have a protective role in shielding the neural arch and spinal cord from injury. Hyperelongation is defined herein as a neural spine fourfold or more taller than the dorsoventral height of the anterior articular surface of the centrum (see Discussion, below), which accords with

previous iguanodontian examples (e.g. Pereda-Suberbiola *et al.* 2011; Gasulla *et al.* 2015; Bertozzo *et al.* 2017).

Hyperelongation of neural spines is rare in extant reptiles but has evolved independently in tetrapods on several occasions. Among extant squamates, hyperelongation is found in three genera: (1) the chamaeleonid *Trioceros cristatus* Stutchbury 1837, in which a sail is present along the dorsal and caudal regions in both male and female specimens, but is more prominent in the male, sometimes with a dip over the sacral region (Klaver & Böhme 1992); (2) the iguanians *Basiliscus basiliscus* Linnaeus 1758, in which the male has a sail along its dorsal and caudal vertebral series (van Devender 1978), and *Basiliscus plumifrons* Cope 1875, in which the male also has head ornamentation (Lattanzio 2019), while in female specimens the crest is very much reduced; and (3) several iguanian agamid sailfin lizards of the genus *Hydrosaurus* Kaup 1828, in which a large caudal sail and a less developed dorsal sail are present, the latter being considerably more prominent in male specimens (Denzer *et al.* 2020). Therefore, in all extant taxa, possession of a sail structure is, to some degree but not exclusively, a male sexually dimorphic character.

In the fossil record, neural spine hyperelongation developed in several clades during the late Carboniferous and Permian. These include sphenacodontids, such as the iconic *Dimetrodon limbatus* Cope 1877 and *Echinerpeton intermedium* Reisz 1972, the latter being the earliest known example in tetrapods (Mann & Reisz 2020). Other examples are the edaphosaurids, such as *Edaphosaurus pogonias* Cope 1882, and a temnospondyl, *Platyhystrix rugosus* Case 1910. During the Triassic, neural spine hyperelongation appeared in rauisuchian archosaurs, including *Arizonasaurus babbitti* Welles 1947 (Nesbit 2003) and *Ctenosauriscus koeneni* Butler *et al.* 2011. Among dinosaurs, the phenomenon was not restricted to ornithomorphs but included theropods and dicraeosaurid sauropods. Theropods are represented by *Altispinax dunkeri* Huene 1923, an early example from the Valanginian Wadhurst Clay Formation (Wealden Group) near Hastings in England, as well as *Acrocanthosaurus atokensis* Stovall & Langstone 1950, *Concavenator corcovatus* Ortega *et al.* 2010, *Spinosaurus aegyptiacus* Stromer 1915, and *Suchomimus tenerensis* Sereno *et al.* 1998, all from the Cretaceous. Sauropods with elongate neural spines include *Dicraeosaurus hansemani* Janensch 1914, *Dicraeosaurus sattleri* Janensch 1914 and *Brachytrachelopan mesai* Rauhut *et al.* 2005, from the Late Jurassic, and *Amargasaurus cazaui* Salgado & Bonaparte 1991 and *Bajadasaurus pronuspinax* Gallina *et al.* 2019 from the Early Cretaceous.

Several theories have been proposed to explain hyperelongation of neural spines in dinosaurs and tetrapods more generally, including a thermoregulatory sail (e.g.

Romer 1948), support for a fat storage reservoir (Romer & Price 1940; Bailey 1997), morphological sexual signalling (e.g. Bertozzo *et al.* 2017) and interspecies signalling (e.g. Huttenlocker *et al.* 2011).

Hyperelongation in the sauropods *Bajadasaurus pronuspinax* and *Amargasaurus cazaui* differs from that in iguanodontians and theropods given that the sauropods have bifid, rod-like neural spines on the cervical vertebrae that curve anterodorsally (Galina *et al.* 2019). These spines would have faced anteriorly with the neck held in flexion, and it has been suggested that they supported a keratin sheath and represent a form of passive defence mechanism (Galina *et al.* 2019). However, the posterior dorsal neural spines remain hyperelongate but cease to be bifid and are markedly transversely expanded, being spatulate in anterior view, but of unknown function (Salgado & Bonaparte 1991).

The function of neural spine hyperelongation in ornithomorphs and theropods was first discussed in detail by Bailey (1997), who recorded a hypothesis, popular at the time, that tall spines supported a sail-like structure used in thermoregulation, based principally on the elongate and subcircular (in cross-section) neural spines of *Dimetrodon* spp. (e.g. Romer 1948; Bramwell & Fellgett 1973; Tracy *et al.* 1986; Florides *et al.* 1999). More recently, this hypothesis for edaphosaurid synapsids was challenged by Huttenlocker *et al.* (2011), who did not find osteohistological evidence to support a significant arterial blood supply to the sail and suggested that a highly vascular, but structurally weak, sail would be potentially lethal if injured and would also generate considerable vascular resistance physiologically. They proposed an intra- or interspecies display function as being the most likely explanation. Others, such as Bennett (1996), showed that the sail of *Edaphosaurus*, with its transversely extending nodules, was well-adapted to allow heat loss by convection. Bony structures may not necessarily be an essential requirement for significant blood flow, given that simply enlarging the surface area may help with thermoregulation, similar to the thermoregulatory cooling effect of the ears in African elephants (Wright 1984). Bailey (1997) noted that *Ouranosaurus nigeriensis* and *Spinosaurus aegyptiacus*, unlike the earlier synapsids, both possessed more blade-like neural spines, used for muscle attachment. He saw similarities between their elongate spines and those found on the anterior thoracic vertebrae of the American bison and proposed that the function in both groups of animals may have been to support a hump. However, the bison's 'hump' is formed predominantly by the robust neck musculature required to support and power its immense head, although the neural spines may also serve to accentuate the height of the animal and are more prominent in male specimens (Meagher 1986). This suggests that they could

also have a secondary intimidatory or morphological sexual signal function. The explanation for neural spine hyperelongation in dinosaurs, which varies from the huge sails of *Spinosaurus aegyptiacus* (Ibrahim *et al.* 2014, 2020) to the strange, elongated spines of only the 11th and 12th dorsal vertebrae in *Concavenator corcovatus* Ortega *et al.* 2010, remains enigmatic, although Thomkins *et al.* (2010) found that in extant taxa, characteristics that have been exaggerated to a degree that exceeds practical function are invariably sexually selected. The current evidence from extant and extinct taxa points to an explanation of very tall neural spines in iguanodontians as either for: morphological sexual signalling (which, according to Padian & Horner (2011), implies that sexual dimorphism is likely); to enhance apparent size, to discourage competition and perhaps predation; or as a means of interspecies visual signalling (this last function usually generating maximal divergence when there are intermediate levels of sympatry (parapatric and peripatric speciation) rather than in areas of allopatry (Padian & Horner 2011; Caro & Allen 2017)). The temporal association of hyperelongation of the neural spines of iguanodontians with a period of presumed increased diversity would support a potential connection with species signalling. However, against this hypothesis, extant species usually have low-cost strategies such as colouration (Caro & Allen 2017), vocalization or other courtship behaviour with little evidence of exaggerated structures being used for this purpose (Hone & Naish 2013).

This paper addresses aspects of neural spine variation in iguanodontians by documenting a new sail-backed taxon from the Wealden Group of the Isle of Wight and exploring the ancestral origins and evolution of neural spine elongation and hyperelongation in iguanodontian dinosaurs.

*Institutional abbreviations.* IWCMS, Isle of Wight County Museum Service (MIWG, Museum of Isle of Wight Geology, was used for accessions prior to 1994), Dinosaur Isle Museum, Isle of Wight, UK; NHMUK, Natural History Museum, London, UK; RBINS, Royal Belgian Institute of Natural Sciences, Brussels, Belgium; USNM, Smithsonian Museum of Natural History (previously the United States National Museum), Washington DC, USA; YPM, Yale Peabody Museum, New Haven, CT, USA.

## GEOLOGICAL SETTING

The Lower Cretaceous Wealden Group strata of southeastern England can be divided into those occupying the more easterly Weald Sub-basin, and those occupying the more south-westerly Wessex Sub-basin, the northern part of which crops out on the Isle of Wight (Radley 2006; Batten & Austin 2011; Sweetman 2011; Gale 2019). The Wealden

Group extends temporally from the Berriasian to the early Aptian (Fig. 1A), but on the Isle of Wight only the younger section, from the late Hauterivian–Barremian boundary to the lower Aptian, is exposed (Fig. 1A). On the Isle of Wight these beds are principally located along the part of the southwest coast that borders Compton Bay, Brook Bay and Brighstone Bay, with a smaller exposure to the east at Yaverland near Sandown (Fig. 1B). The Wessex Formation is known for its vertebrate-rich plant debris beds (*sensu* Oldham 1976; see Sweetman & Insole 2010) which, despite representing only a tiny fraction of the overall succession, yield the vast majority of dinosaur remains that are recovered from the island, including the specimen described herein. Sweetman & Insole (2010, p. 409) interpreted plant debris beds as representing a ‘locally generated sheet flood, which was then transformed on the floodplain into a debris flow by the acquisition of surface material’. For a more detailed description of the Isle of Wight Wealden Group see Martill and Naish (2001), Batten (2011), Gale (2019) and Lockwood *et al.* (2021 and references therein).

## MATERIAL & METHOD

### Neural spine height data

There is no absolute consensus on how to measure various elements of a vertebra, which can lead to slight differences in the metrics obtained between different authors. In this study the dorsoventral height of the neural spine was measured from the level of the ventral-most margin of the postzygapophyseal facet in lateral view to the dorsal-most (distal) tip of the spine, a method that also facilitated the use of images in data collection. Width of the neural spine was recorded as the maximum anteroposterior diameter in its dorsal half. Dorsoventral height of the centrum was measured on the anterior articular surface. When the position of the vertebra was not known it was estimated by the size and position of the parapophyses and the angles of the transverse processes compared with those in known complete dorsal vertebral spines (Norman 1980, 1986; Forster 1990; Bonser *et al.* 2023; Lockwood *et al.* 2024). Posterior dorsal centra tend to become taller in iguanodontians and the neural spines also usually become taller (Norman 1980, 1986; Forster 1990), meaning that the ratio between the two remains fairly stable along this section of the column.

Relative height of the neural spine is expressed as the ratio of the neural spine height to the height of the centrum using the anterior articular surface (Nh/Ch ratio), and the gracility index as the ratio of the neural spine height to its anteroposterior width (Nh/Nw ratio).

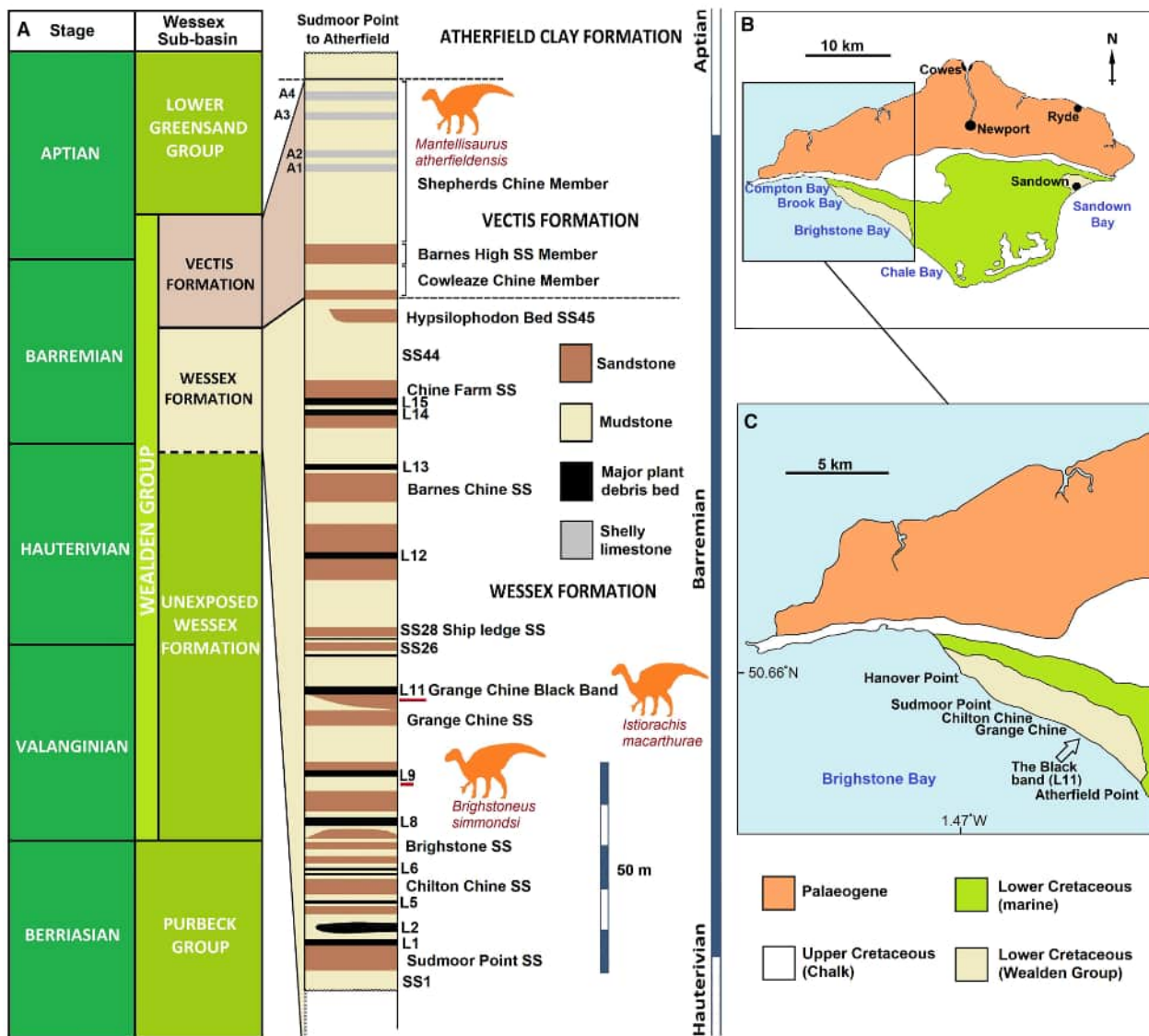


**FIG. 1.** Locality and stratigraphy of *Istiorachis macarthurae* gen. et sp. nov. A, generalized stratigraphic log modified from Allen & Wimbledon (1991); schematic lithological logs of Wealden Group exposure between Sudmoor and Atherfield on the Isle of Wight adapted from Sweetman (2007), showing excavation sites of the holotypes of the new dinosaur described herein (MIWG 6643), *Brighstoneus simmondsi* (MIWG 6344) and *Mantellisaurus atherfieldensis* (NHMUK PV R 5764). B, simplified geological map of the Isle of Wight. C, enlarged area showing the site of the excavation of MIWG 6643 in the Black Band (arrowed) (50.63354 N, 1.40654 W). Abbreviation: SS, sandstone. Note that the dashed line in A dividing the Wessex Formation into exposed and unexposed, applies only to the Isle of Wight exposures.

A database of iguanodontian neural spine metrics was compiled largely from published photographs, drawings and reconstructions, with photographs possibly underestimating the height slightly in taller neural spines due to extension distortion, and reconstructions producing indicative rather than precise results. Given that the status of ‘*Dollodon bampingi*’ is controversial (Norman 2012; McDonald 2012a) it is referred to

herein by its specimen number (RBINS R57) instead. Mass estimations were largely calculated using the regression equation developed for Ornithischia by O’Gorman & Hone (2012) based on femoral lengths, which were mainly obtained from Benson *et al.* (2014). Data were also collected from Paul (2016) and others. The full dataset is available in Dryad (Lockwood *et al.* 2025).



### Phylogeny

Phylogenetic relationships were assessed using the matrix of Lockwood *et al.* (2024) with the addition of two taxa, *Istiorachis macarthurae* and *Morelladon beltrani*, and an additional character, character 126: ratio of neural spine dorsoventral height from postzygapophyseal facet to dorsal margin and the dorsoventral height of the anterior articular surface of the centrum of posterior series dorsal vertebrae: (0) ratio <2, (1) ratio  $\geq 2$  and <3, (2) ratio  $\geq 3$  and <4, (3) ratio  $\geq 4$  (see Appendix S1 for further details; the phylogenetic matrix is available in Appendix S2). This gave a matrix of 44 taxa and 126 unordered characters. The matrix of Lockwood *et al.* (2024) was a modified version of the matrix of Xu *et al.* (2018), which itself was modified from Norman (2015) and McDonald (2012b). The matrix was chosen because it covers early diverging iguanodontians without being overly focused on hadrosaurids. The matrix was compiled in Mesquite v. 3.61 (Maddison & Maddison 2015) and analysed in TNT v. 1.6 (Goloboff & Morales 2023). *Lesothosaurus diagnosticus* was set as the outgroup.

First, the data matrix was analysed using the traditional search algorithm using tree bisection–reconnection (TBR) branch swapping, saving 1000 trees per replication. A second analysis was performed using extended implied weighting (Goloboff 2014) with a concavity constant (k) of 3 in order to downweigh homoplastic characters. A new-technology search was carried out using the sectorial search, ratchet, drift and tree-fusing algorithms maintaining defaults. Trees were obtained from a random addition sequence. An additional round of TBR branch swapping was then carried out on trees held in memory to obtain all of the most parsimonious trees (MPTs).

Consistency index, rescaled consistency index and retention index were calculated using the TNT script STATS.RUN and clade support using the TNT script BREMER.RUN and TNT bootstrap, set to 1000 replicates, reporting groupings found in >50% of pseudoreplicate datasets.

### Neural spine ancestral state reconstruction

Ancestral states for neural spine elongation were investigated using the MPT recovered from the extended implied weights analysis. First, the tree was time-calibrated using the TimePaleoPhy function in the R package paleotree (v3.4.7; Bapst 2012), with minimum branch lengths of 0.5 myr. Taxa without neural spine data were then pruned. Ancestral states of posterior dorsal vertebrae neural spine heights, expressed as ratios to anterior centrum height (Nh/Ch ratio) were calculated using the anc.ML function in the R package phytools (v2.4.4; Revell 2024), which uses a Brownian motion

model of evolution and maximum likelihood. All analyses were carried out in R v4.0.4 (R Core Team 2021). For data and script see Lockwood *et al.* (2025).

## SYSTEMATIC PALAEOLOGY

DINOSAURIA Owen 1842

ORNITHISCHIA Seeley 1888

ORNITHOPODA Marsh 1881

IGUANODONTIA Baur 1891

ANKYLOPOLLEXIA Sereno 1986

STYRACOSTERNA Sereno 1986

Genus *Istiorachis* nov.

LSID. <https://zoobank.org/NomenclaturalActs/e68743c5-8ab0-4185-abd4-666b2c7d4d96>

*Derivation of name.* The name is derived from the Ancient Greek words ἰστίον (*istion*), meaning a sail, and ράχης (*rachis*), the spine or backbone. It refers to the probable sail-back appearance of the dinosaur.

*Type species.* *Istiorachis macarthurae* gen. et sp. nov.

*Diagnosis.* As for type and only species.

*Istiorachis macarthurae* sp. nov.

Figures 3–15

LSID. <https://zoobank.org/NomenclaturalActs/0f175f3b-6cb2-4739-806d-81be81ba4c38>

*Derivation of name.* The species name honours Dame Ellen MacArthur, an English sailor who in 2005 set a world record for the fastest solo non-stop voyage around the world on her first attempt and who also founded the Ellen MacArthur Cancer Trust for young people on the Isle of Wight.

*Holotype.* MIWG 6643 is a partial skeleton composed of the following elements: one cervical vertebra, eight dorsal vertebrae, three dorsal rib heads, a partial sacrum, seven caudal vertebrae, both pubes and both ischia.

*Location & horizon.* MIWG 6643 was excavated by the late Mr Nicholas Chase from the 'Black Band' (bed L11 in Stewart 1978), a plant debris bed cropping out c. 100 m east of Grange Chine, lying above the Grange Chine Sandstone in the Wessex Formation. The site is a c. 1.5-m-thick bed that has occasionally yielded dinosaur remains, including IWCMS 1997.550, the holotype specimen of the tyrannosauroid theropod *Eotyrannus lengi* (Hutt *et al.* 2001; Naish & Cau 2022). Unfortunately the excavation site was poached and an unknown amount of the skeleton was taken before collection could be completed.

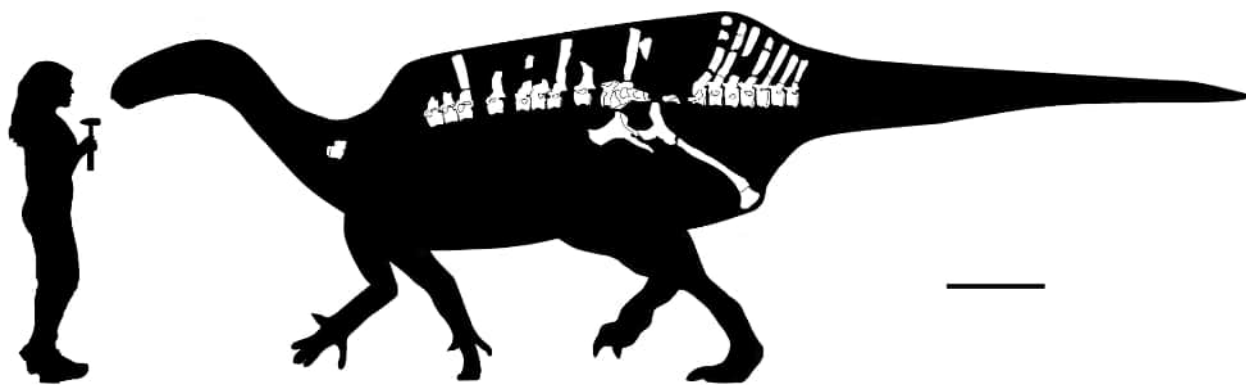


**FIG. 2.** *Istiorachis macarthurae* gen. et sp. nov. holotype (MIWG 6643). Skeletal reconstruction. Scale bar represents 500 mm.

**Diagnosis.** *Istiorachis macarthurae* differs from all other iguanodontians by possessing one autapomorphy, namely two anterior parasagittal tuberosities present on the ventral surface of a posterior dorsal vertebra, marking a change from vertebrae with a ventral keel to a flat surface. A posterior cervical vertebra has a damaged anteroventral process at the base of the neural spine, potentially representing a second autapomorphy. *Istiorachis macarthurae* also possesses the following features, which, although not unique to the taxon, occur in a unique character combination. An interpostzygapophyseal fossa and tubular cavity is located between the origin of the postzygapophyses and above the neural canal: a similar fossa is also seen in *Lesothosaurus diagnosticus* (Baron *et al.* 2017), *Camptosaurus dispar* (Gilmore 1909), *Iani smithi* (Zanno *et al.* 2023), *Mantellisaurus atherfieldensis* (NHMUK PV R 5764), *Tanius sinensis* (Borinder *et al.* 2021) and *Eolambia caroljonesa* (McDonald *et al.* 2012). A strongly developed centro-postzygapophyseal lamina is present, especially in the anterior dorsal vertebrae. Dorsal neural spines hyperelongated to over fourfold the height of the anterior articular surface of the centrum, as also occurs in the non-hadrosaurids *Ouranosaurus nigeriensis* (Taquet 1976) and *Morelladon beltrani* (Gasulla *et al.* 2015). Ischium with sinusoidal shaft in lateral view, as also seen in *Bactrosaurus johnsoni* (Godefroit *et al.* 1998) and *Gilmoresaurus mongoliensis* (Prieto-Márquez & Norell 2010). Ischium with strongly developed distal boot with an anteroposterior diameter 3.3-fold as wide as the midshaft, as also seen in *Bactrosaurus johnsoni* (Godefroit *et al.* 1998) and *Eolambia caroljonesa* McDonald *et al.* 2012).

## OSTEOLOGICAL DESCRIPTION

MIWG 6643 is in good condition, with little distortion and good surface preservation. Elements from the axial spine and pelvis are preserved (Fig. 2). Comprehensive photographs and measurements of all axial and pelvic elements are available in Appendix S1 (Figs S1–S26; Tables S1–S6).

### Cervical vertebra

A single cervical vertebra (Fig. 3) is preserved but is missing the postzygapophyses and distal transverse processes.

In right lateral view the body of the centrum, excluding the convex anterior articular surface, is anteroposteriorly elongate (ratio of length to height = 1.4) and slightly concave ventrally (Fig. 3C). In *Mantellisaurus atherfieldensis* (NHMUK PV R 5764) and *Iguanodon bernissartensis* (RBINS R51) the cervical vertebrae are essentially equidimensional in lateral view, whereas in other iguanodontians they may all be rectangular (long axis anteroposterior), as in *Camptosaurus dispar* (Carpenter & Wilson 2008), or elongate only in the anterior section of the series, as in *Tenontosaurus tilletti* (Forster 1990) and *Comptonatus chasei* (Lockwood *et al.* 2024). The surface of the lateral wall of the centrum is divided by an anteroposteriorly oriented lateral ridge (Fig. 3C; lar), anterior to which is a damaged parapophysis. The neurocentral synchondrosis is visible. The anterior articular surface is convex and lacks a definite notochordal pit, although the central area is damaged (Fig. 3A). The posterior articular surface is deeply concave with a slightly everted margin (Fig. 3B). Ventrally a broad, anteroposteriorly extending keel is present, which is further expanded transversely in its posterior section and merges with the posteroventral articular margin (Fig. 3F; vk). The neuropophyses support robust transverse processes with dorsomedially facing prezygapophyseal facets on their dorsal surfaces (Fig. 3D; prez). The facets have migrated well away from the neural arch, which suggests that the vertebra was situated posteriorly in the column. The neural spine is incomplete dorsally, but the fractured cross-section suggests that it was probably a small, transversely compressed nubbin of bone. An incomplete process projects anteriorly from the anterior margin of the neural spine base and overhangs the neural arch (Fig. 3G–H; apr). One or more postaxial cervical vertebrae are preserved in several non-hadrosaurid iguanodontians. However, in most taxa the series is incomplete and the neural spine, when present, is frequently damaged. An anterior process at the base of the neural spine is not reported in the description of postaxial cervical vertebrae from any non-hadrosaurid

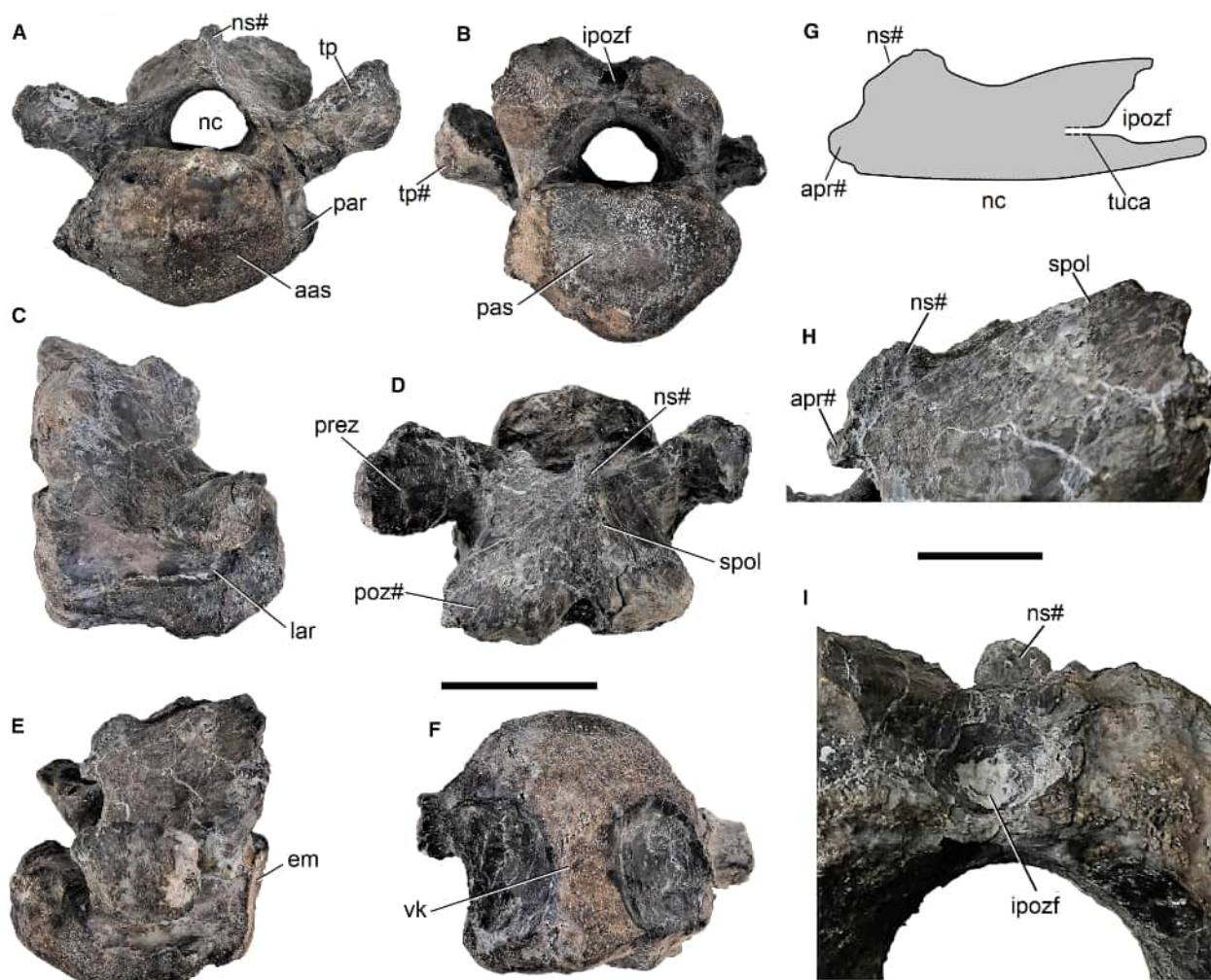


**FIG. 3.** *Istorachis macarthurae* gen. et sp. nov. holotype (MIWG 6643). Cervical vertebra in: A, anterior; B, posterior; C, right lateral; D, dorsal; E, left lateral; F, ventral view. G, sagittal cross-section of neurapophyses, dorsal to neural canal. H, close up of neural spine in left lateral view. I, close up of interpostzygapophyseal fossa and tubular cavity in posterior view. *Abbreviations:* aas, anterior articular surface; apr, anterior process; em, everted margin; ipozf, interpostzygapophyseal fossa; lar, lateral ridge; nc, neural canal; ns, neural spine; par, parapophysis; pas, posterior articular surface; poz, postzygapophysis; prez, prezygapophysis; spol, spinopostzygapophyseal lamina; tp, transverse process; tuca, tubular cavity; vk, ventral keel, #, fracture surface or feature partially broken. Scale bars represent 50 mm.

iguanodontian, even those with better preservation such as *Tenontosaurus tilletti* (Forster 1990), *Camptosaurus dispar* (Gilmore 1909), *Uteodon aphanoecetes* (Carpenter & Wilson 2008), *Iguanodon bernissartensis* (Norman 1980), *Mantellisaurus atherfieldensis* (Bonsor et al. 2023), *Bactrosaurus johnsoni* (Godefroit et al. 1998), *Eolambia caroljonesa* (McDonald et al. 2012) and *Taninus sinensis* (Borinder et al. 2021), which all possess neural spines that are a low, laterally compressed tab or low ridge. There are moderately developed spinopostzygapophyseal laminae in *Istorachis macarthurae* extending from the neural spine to the fractured bases of the postzygapophyses (Fig. 3D, H; spol). Posterior to the junction of the

postzygapophyses there is a depressed area (interpostzygapophyseal fossa) that is separated by a slightly damaged, thin shelf from the neural canal, and continues anteriorly into a small calcite-filled tubular cavity with a circular entrance (diameter c. 2 mm), that extends anteriorly into the neural arch for at least 5 mm (Fig. 3G, I; ipozf). An interpostzygapophyseal fossa is seen in other taxa, such as *Lesothosaurus diagnosticus* (Baron et al. 2017), *Iani smithi*, (Zanno et al. 2023), *Camptosaurus dispar* (Gilmore 1909), *Mantellisaurus atherfieldensis* (NHMUK PV R 5764), *Taninus sinensis* (Borinder et al. 2021) and *Eolambia caroljonesa* (McDonald et al. 2012), although in some it is more of a shelf extending anteriorly between the bases of



the postzygapophyses, as in *Hypselospinus fittoni* (Norman 2015), rather than a pit. In others it appears to be absent (e.g. *Ouranosaurus nigeriensis* (Bertozzo *et al.* 2017) and *Gobihadros mongoliensis* (Tsogtbaatar *et al.* 2019)), although it may be that the feature is present only in the more or most posterior vertebrae. Gilmore (1909, p. 230) on *Camptosaurus* spp. described 'posteriorly just below the junction of the posterior zygapophyses is a pit-like foramen leading forward into the neural process'. This is present in all cervical vertebrae of the type specimen (YPM VP 001877), USNM 4282 and USNM 5474, but entirely absent in USNM 5473. It is difficult to know whether the anteriorly projecting process on the anterior margin of the neural arch and the interpostzygapophyseal fossa are more widely represented in iguanodontians because this area is sometimes poorly preserved and not described and/or figured in some taxa. In *Istiorachis macarthurae* the fossa and process appear to be in alignment. In articulated iguanodontian cervical vertebral series, the anterior convex articular surface of the centrum is seated in the posterior concavity of the preceding vertebra such that it is almost completely obscured in lateral view; for example, *Mantellisaurus atherfieldensis* (Bonsor *et al.* 2023), *Iguanodon bernissartensis* (Norman 1980) and *Jinzhousaurus yangi* (Wang *et al.* 2010). As can be seen in the dorsal view of the cervical vertebra of *Istiorachis macarthurae* (Fig. 3D), if the anterior convexity was removed and if similar adjacent vertebrae were in articulation, the process and fossa would have been in extremely close proximity, perhaps forming a peg-and-socket articulation. The possible function of this feature is discussed below, although we regard the anterior process at the base of the neural spine to be potentially autapomorphic to *Istiorachis macarthurae*.

#### Dorsal vertebrae

Eight dorsal (D) vertebrae are preserved and have been given provisional numbers based on their probable order, assuming a total count of 17 including the sacrodorsal vertebra, and based on comparisons with early diverging iguanodontians with complete dorsal spines such as *Tenontosaurus tilletti* (Forster 1990), *Mantellisaurus atherfieldensis* NHMUK PV R 5764, RBINS R57 (Norman 1986) and *Iguanodon bernissartensis* (Norman 1980). This estimated sequence number is used in the description for guidance: D4–6, anterior; D8, middle; D10–12, posterior; and D14, posteriormost.

All of the vertebral centra are longer anteroposteriorly than tall dorsoventrally except D14, for which the posterior articular face is 1 mm (1.25%) taller than the length of the centrum (Table 1).

*Anterior dorsal vertebrae.* D4–D6 appear to be an articulated sequence (Fig. 4A–H). The articular surfaces are dorsoventrally taller than transversely wide and are flat to very slightly concave. The dorsal margins of the anterior and posterior articular surfaces are almost straight and horizontal, while the gently everted lateral and ventral margins form a U shape. In lateral view the ventral margin of the centrum is gently concave, while the lateral surfaces are flat dorsoventrally but concave anteroposteriorly, forming a spool shape in ventral view (Fig. 4G). Ventrally there is a longitudinal keel (Fig. 4G; vk) which is less prominent in D6. The anterior and posterior margins of the centrum, especially on the ventral surfaces, are very rugose, this being formed by a series of deep longitudinal grooves (Fig. 4G; rug). Neurocentral synchondroses are clearly visible on the dorsal half of the lateral walls. The centrum supports the neurapophyses, which enclose large neural canals. Anteriorly, the prezygapophyses have dorsomedially facing facets that only just overhang the anterior articular surface in lateral view (Fig. 4B; prez). Posterior to the prezygapophyses are oval parapophyses (long axis directed anteroventrally). Extending down the dorsal column, the size of the parapophyses diminishes and they migrate dorsally so that in D6 they abut the base of the transverse process.

The transverse processes are triangular in cross-section with the apex directed ventrally. The dorsal surface is smooth and slightly convex anteroposteriorly. Proximally, the ventral apex is formed by the robust posterior centrodiapophyseal lamina (Fig. 4D; pcdl), which forms the lateral wall of a deep recess on the neural arch in posterior view. This recess is bounded medially by a considerably less robust postzygodiapophyseal lamina (Fig. 4D; podl), and ventrally by a particularly strongly developed centropostzygapophyseal lamina (Fig. 4D; cpol). The latter appears more robust than in the sympatric *Mantellisaurus atherfieldensis* and *Brighstoneus simmondsi*. The posterior recess also extends laterally so that the posteroventral surface of the transverse process is anteroposteriorly concave. The dorsomedial surface of the posterior recess blends almost continuously, but with a small step, with the ventrolaterally facing facet of the postzygapophysis. The transverse processes of D4–6 are directed posterolaterally in dorsal view (Fig. 4C) and dorsolaterally in D4 and D5 in anterior view, becoming more horizontal in D6. The neural spines are all incomplete, although the angle of fracture and preservation of a loose spine means that it may be associated with D6. The fractured cross-sections of the neural spines show a transversely compressed ellipse. Anteriorly, the ventral section of the neural spine becomes a thin blade of bone extending between the prezygapophyses. A shallow cleft separates the postzygapophyses posteriorly but unlike *Morelladon beltrani* (Gasulla



**TABLE 1.** Metrics (in mm) of *Istiorachis macarthurae* gen. et sp. nov. (MIWG 6643) axial elements.

Vertebra	Anterior height	Anterior width	Posterior height	Posterior width	Length	NS height	NSh/Ch	Approx. position
Cervical	52	64	51	80	86			Posterior
Dorsal (1)	72	60	67	58	81			D4
Dorsal (2)	68	59	69	62	79			D5
Dorsal (3)	72	60	68	61	83			D6
Dorsal (4)	67	57	65	66	85			D8
Dorsal (5)	67	63	71	72	82			D10
Dorsal (6)	71	69	71	75	83			D11
Dorsal (7)	71	77	69	71	76	305	4.3	D12
Dorsal (8)	74	83	81	95	80			D14
Sacrodorsal	81	110	91	130	69			SD
S1	91	130		64	79			S1
S2		64		62	80			S2
S3		62						S3
S4/5		68		68				S4/5
Caudal (1)	77	90	83	102	75			SC (Cd1)
Caudal (2)	88	96	86	96	74	201+		Cd2
Caudal (3)	92	103	86, 96	89	75			Cd3
Caudal (4)	86, 99	80	84, 99	77	79			Cd7
Caudal (5)	77, 87	75	79, 91	77	75	268	3.5	Cd5
Caudal (6)	74, 85	74	76, 88	72	79	210	2.4	Cd4
Caudal (7)	74, 84	73(e)	73, 85	70	77	182+	2.4+	Cd6

Approximate position of vertebrae assumes that MIWG 6643 originally possessed 16 dorsal vertebrae plus a sacrodorsal. An antero-posteriorly narrow dorsal neural spine (height 196 mm) may be associated with D6 based on fracture shape and preservation. This would give a neural spine height : anterior articular surface of centrum height ratio of 3.9+. An isolated incomplete sacral neural spine is 297 mm in height. In the Cd1 reconstruction the Nh/Ch ratio is 4.0+. Heights of the anterior and posterior articular surfaces of Cd3–7 are given with and without haemal facets. Cd1 may be considered a sacrocaudal (SC) vertebra. Ch, height of the centrum using the anterior articular surface; (e), estimated measurement; NS, neural spine; NSh, neural spine height.

*et al.* 2015), it does not extend dorsally up the posterior margin of the neural spine.

**Mid-dorsal vertebra.** D8 (Fig. 4I–L) is similar to the anterior vertebrae in most respects but differs in the following ways. The transverse processes are posterolaterally directed (Fig. 4J), but less posteriorly oriented than in the more anterior vertebrae. The parapophyses are smaller and have migrated onto the proximal part of the anterior margins of the transverse processes (Fig. 4I, K; para). The facets of the prezygapophyses face dorsomedially but are more horizontal than in the anterior vertebrae.

**Posterior dorsal vertebrae.** D10–D12 articulate with each other. The vertebrae are similar in most respects to the mid-dorsal vertebrae, differing only in the following respects. In D10 and D11 the anterior articular surface is flat and dorsoventrally taller than transversely wide, as in the anterior dorsal vertebrae, but the posterior surface is wider transversely than tall, while in D12 (Fig. 5A, C) both surfaces are wider than tall (Table 1). The shape of the articular surfaces has changed from being U shaped

to circular, the change occurring earlier in the posterior surface. D10 has a ventral keel, but this is absent in D11 and D12. Excluding the sacrodorsal vertebra, ventral keels are found in all the dorsal vertebrae of *Zalmoxes shqiperorum* (Godefroit *et al.* 2009), *Camptosaurus dispar* (Gilmore 1909), *Uteodon aphanoeetes* (Carpenter & Wilson 2008, described as *Camptosaurus* therein), *Ouranosaurus nigeriensis* (Bertoizzo *et al.* 2017), *Mantellisaurus atherfieldensis* (NHMUK PV R 5764), *Iguanodon bernisartensis* (Norman 1980), *Comptonatus chasei* (Lockwood *et al.* 2024), *Brachylophosaurus canadensis* (Prieto-Márquez 2001), and probably *Bactrosaurus johnsoni* (Godefroit *et al.* 1998) and *Edmontosaurus regalis* (Lambe 1920). *Cumnoria prestwichii* lacks a ventral keel on any of the anterior or posterior vertebrae (Maidment *et al.* 2023). Among other taxa, all but the most posterior dorsal vertebrae are probably keeled in *Hypselospinus fittoni* (Norman 2015); *Morelladon beltrani* has three preserved dorsal centra in estimated positions D8, 11 and 12, which all possess keels (Gasulla *et al.* 2015); *Brighstoneus simmondsi* has keeled dorsal vertebrae from the anterior, middle and posterior series, but one posterior centrum lacks a keel;

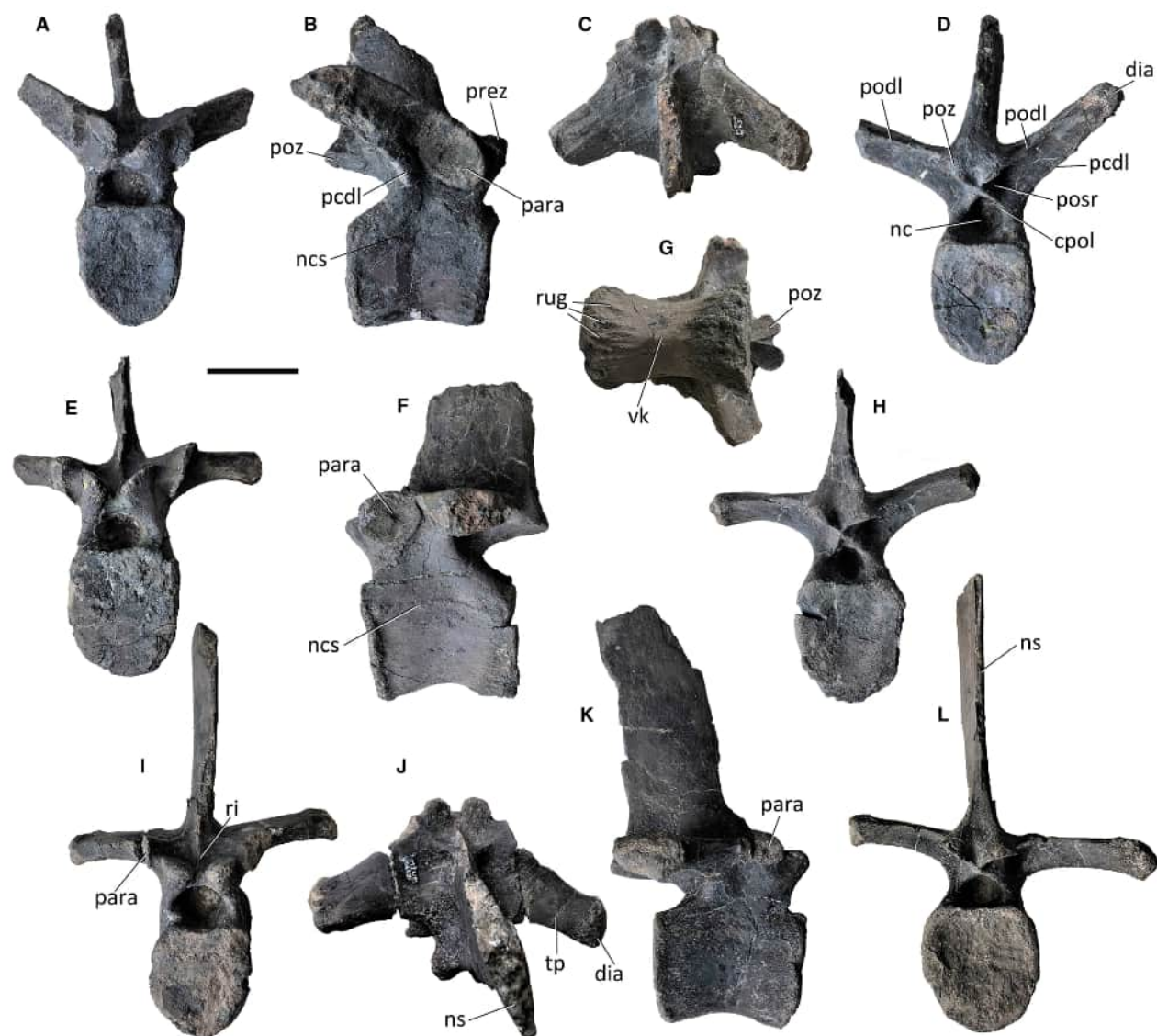


**FIG. 4.** *Istiorachis macarthurae* gen. et sp. nov. holotype (MIWG 6643). Anterior and middle dorsal vertebrae. A–D, 4th dorsal vertebra in: A, anterior; B, right lateral; C, dorsal; D, posterior view. E–H, 6th dorsal vertebra in: E, anterior; F, left lateral; G, ventral; H, posterior view. I–L, 8th dorsal vertebra in: I, anterior; J, dorsal; K, right lateral; L, posterior view. *Abbreviations:* cpol, centropostzygapophyseal lamina; dia, diapophysis; nc, neural canal; ncs, neurocentral synchondrosis; ns, neural spine; para, parapophysis; pcdl, posterior centrodiapophyseal lamina; podl, postzygodiapophyseal lamina; posr, posterior recess; poz, postzygapophysis; prez, prezygapophysis; ri, ridge; rug, rugosity; tp, transverse process; vk, ventral keel. Scale bar represents 50 mm.

and the four preserved dorsal vertebrae from *Magnamimus soriaensis*, probably from the middle series, also lack ventral keels (Fuentes Vidarte *et al.* 2016). Keels restricted to anterior vertebrae but absent posteriorly are seen in *Jinzhousaurus yangi*, in which they are present in D4 and D5 but not in D12 (Wang *et al.* 2010), and *Lesothosaurus diagnosticus* (Baron *et al.* 2017) but, given that the dorsal spine is incomplete in both, the transition area is not known.

In *Istiorachis macarthurae*, between D10 and D12 there appears to be a transitional stage (Fig. 6A–B). Although

the exact position of this sequence is not known with certainty, the close fit of the vertebrae and position of the parapophyses make it highly likely that the actual sequence is correct. In D10 the lateral walls of the centrum curve ventrally to give a transversely convex ventral surface with a strong midline ventral keel. The anterior and posterior margins of this vertebra are also highly rugose (as they are in most of the dorsal vertebrae), due to a series of longitudinal grooves. The subsequent vertebra D11 has two prominent tuberosities placed parasagittally against the anterior margin of the ventral surface,

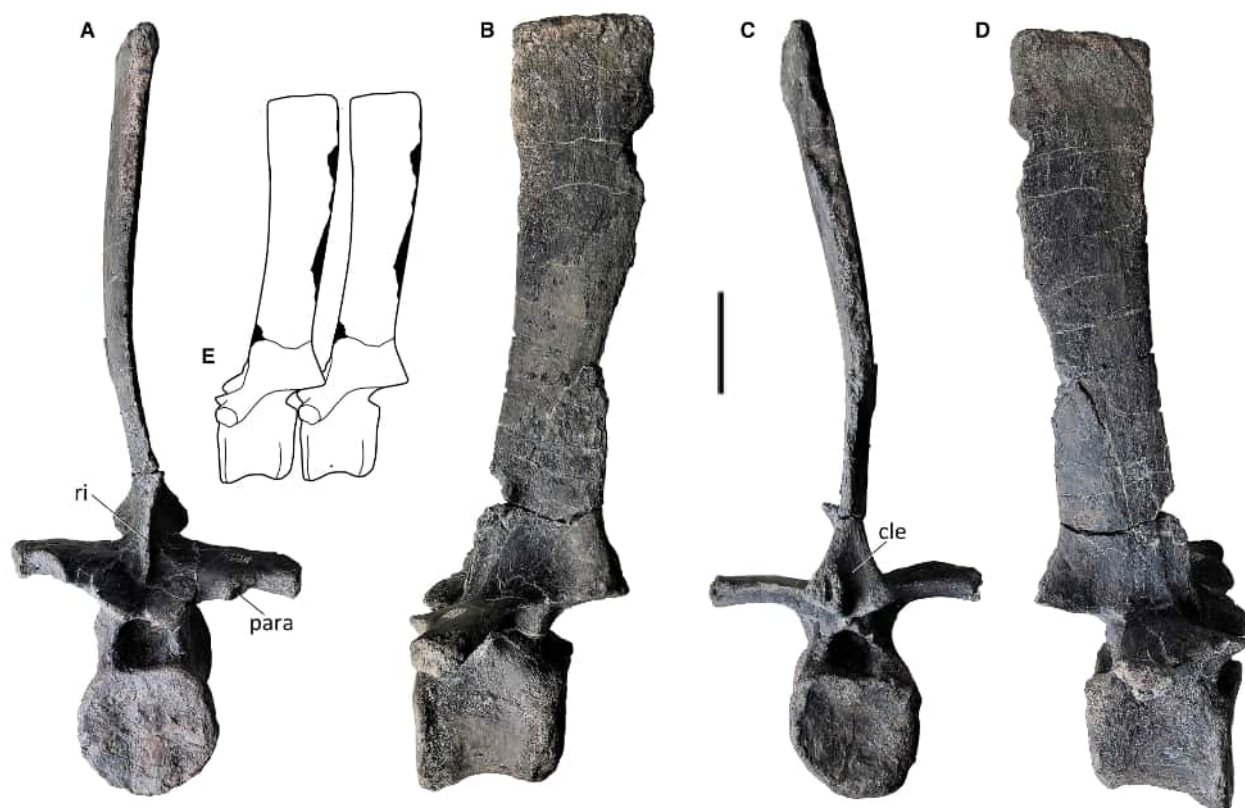


**FIG. 5.** *Istiorachis macarthurae* gen. et sp. nov. holotype (MIWG 6643). 12th dorsal vertebra from early posterior series. A–D, 12th dorsal vertebra in: A, anterior; B, left lateral; C, posterior; D, right lateral view. E, reconstruction to show two consecutive vertebrae in lateral view. Abbreviations: cle, cleft; para, parapophysis; ri, ridge. Scale bar represents 50 mm.

with a sulcus between them (reminiscent of the posterior haemal facet in some iguanodontian caudal vertebrae). The surface is still transversely convex but lacks a keel, and rugosity is largely confined to the posterior margin. Vertebra D12 has a very flat surface, lacking a keel and having much reduced rugosity, although there is some abrasion to the articular margins. The margins between the ventral and lateral surfaces of the centrum are quite angular although this may have been exaggerated by taphonomic distortion and fracture on the right side (Fig. 6B; dis). As far as can be determined, a transition from a keeled ventral surface to a flat one via two tuberosities has not been described previously for other iguanodontians including *Iguanodon bernissartensis* (Norman 1980), *Mantellisaurus atherfieldensis* (Bonsor et al. 2023) and *Comptonatus chasei* (Lockwood et al. 2024). We regard the dorsal vertebra with anterior tuberosities as autapomorphic for *Istiorachis macarthurae*.

The taxonomic utility of ventral keels in iguanodontians has yet to be fully established. In dorsal vertebrae they are not commonly used in phylogenetic studies, although the presence or absence of a ventral keel in the anterior or middle dorsal vertebrae has been used by

Poole (2015, char. 163; 2022, char. 163). The transition series in *Istiorachis macarthurae* showing the keel ending against two tuberosities, presumably acting as osteological correlates, suggests that the keel in iguanodontians is not a random variable but linked to a morphological structure.

In dorsal view, the transverse processes extend laterally at right angles to the sagittal plane, while in anterior view they are horizontal but slightly curved with a gently concave ventral margin. The parapophyses are much smaller than in the anterior dorsal vertebrae and have migrated increasingly laterally onto the transverse processes (Fig. 5A; para). The posterior centrodiapophyseal laminae are less robust and consequently the posterior recesses are less deep. The angle between the facets on the prezygapophyses and postzygapophyses is more obtuse.

D12 has an intact neural spine with slight losses to the posterior margin (Fig. 5). In lateral view (Fig. 5B, D) the neural spine extends almost vertically but has a very gently concave anterior margin and the anteroposterior width of the distal spine is slightly greater than it is proximally. The cross-section is elliptical, but the anterior edge is thinner than the posterior edge, although both



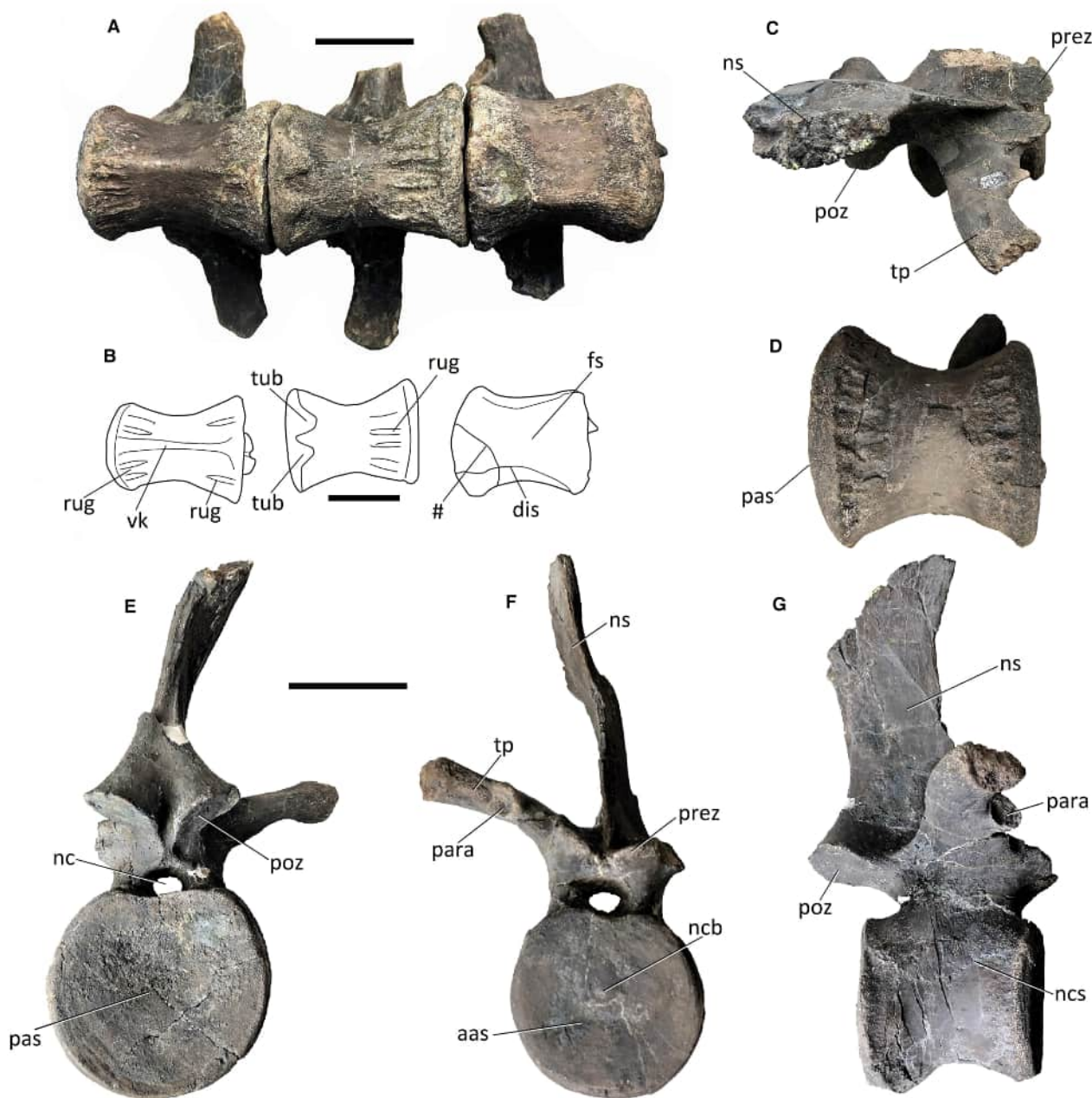


**FIG. 6.** *Istorachis macarthurae* gen. et sp. nov. holotype (MIWG 6643). Posterior dorsal vertebrae. A–B, dorsal vertebrae 10–12 in ventral view: A, photograph of vertebrae in articulation; B, drawings of individual vertebral centra. C–G dorsal vertebra 14 in: C, dorsal; D, ventral; E, posterior; F, anterior; G, right lateral view. *Abbreviations:* aas, anterior articular surface; dis, distortion; fs, flat surface; nc, neural canal; ncb, notochordal boss; ns, neural spine; para, parapophysis; pas, posterior articular surface; poz, postzygapophysis; prez, prezygapophysis; rug, rugosity; tp, transverse process; tub, tuberosity; vk, ventral keel; #, line of fracture. Scale bars represent 50 mm.

become transversely thicker distally. The anterior margin extends between the prezygapophyses as a thin blade of bone (Fig. 5A; ri), while posteriorly it continues as a cleft between the postzygapophyses (Fig. 5C; cle). D12 has an Nh/Ch ratio of 4.3. This differs from the posterior dorsal vertebral neural spines of other Wealden Group

iguanodontian taxa such as *Barilium dawsoni* (Nh/Ch = 2.6), *Hypselospinus fittoni* (Nh/Ch = 3.7), *Comptonatus chasei* (Nh/Ch = 2.6), *Brighstoneus simmondsi* (Nh/Ch = 3.3) and *Iguanodon bernissartensis* (Nh/Ch = 2.1). The neural spines in *Mantellisaurus atherfieldensis* and *Valdosaurus canaliculatus* are not preserved



but the latter had short caudal neural spines and was likely to be similar to other dryosaurids such as *Dryosaurus altus* (Janensch 1955) with an Nh/Ch ratio of 1.0. *Morelladon beltrani* (Nh/Ch = 4.1) from Spain has a similar Nh/Ch ratio to *Istiorachis macarthurae* although the autapomorphic long vertical groove, extending dorsally up the neural spine from between the postzygapophyses, is not present in *Istiorachis macarthurae*.

**Posteriormost dorsal vertebra.** The centrum of D14 is the largest and most robust of the preserved dorsal vertebrae and has deeply anteroposteriorly incised grooves, which increase the rugosity of the lateral surface adjacent to the everted margins of the anterior and posterior articular surfaces. The anterior articular surface is circular with a flattened dorsal margin and is essentially flat, although a small notochordal boss is present at its centre. Among iguanodontians, notochordal bosses are also described in some of the dorsal vertebrae of *Zalmoxes robustus* (Weishampel et al. 2003), *Iguanodon bernissartensis* (Norman 1980) and *Brighstoneus simmondsi* (Lockwood et al. 2021). The posterior articular surface is rounded but with a flattened dorsal margin, and mildly concave. The ventral surface of the centrum is transversely convex but smooth, lacking a keel. The preserved transverse process is gently curved and angled anterolaterally in dorsal view (Fig. 6C; tp), and dorsolaterally in anterior view (Fig. 6F; tp). Its cross-section is oval (long axis anteroposterior), with a less prominent posterior centrodiapophyseal lamina than in preceding vertebrae. The neural spine is incomplete but has a transversely narrow anterior margin and a thicker posterior margin. There is a shallow cleft between the postzygapophyses that continues dorsally up the ventral section of the posterior margin of the neural spine for c. 40 mm, but is not as pronounced or

extensive as observed in *Morelladon beltrani* (Gasulla et al. 2015).

#### Dorsal ribs

The proximal ends of three left dorsal ribs are preserved (Fig. 7), which have a similar morphology to other Wealden Group iguanodontians including those of *Iguanodon bernissartensis*, *Mantellisaurus atherfieldensis* and *Brighstoneus simmondsi*.

The capitula are all damaged but the tubercula are nearly circular and raised on a short pedestal. Anteriorly a broad ridge arises at the level of the tuberculum, that is smoothly rounded transversely and extends down the shaft of the rib. Posteriorly a groove develops ventral to the lateral aspect of the tuberculum and extends down the shaft, separated from the lateral margin by a narrow ridge. This groove was presumably for the neurovascular bundle.

#### Sacrum

A partial sacrum is preserved in two pieces, one consisting of the anterior section, containing the sacrodorsal, sacral (S) 1, S2 and the anterior part of S3 (Fig. 8), and the other, a fragment representing the ventral surface of a more posterior sacral (Fig. 9E). An isolated vertebra probably represents a sacrocaudal and is described with the caudal vertebrae, below.

The anterior articular surface of the sacrodorsal vertebra (Fig. 8D; aas) is wider transversely than tall dorsoventrally, both dimensions being greater than found in the preceding dorsal vertebrae. The margin is everted and slightly indented dorsally by the neural canal, while the

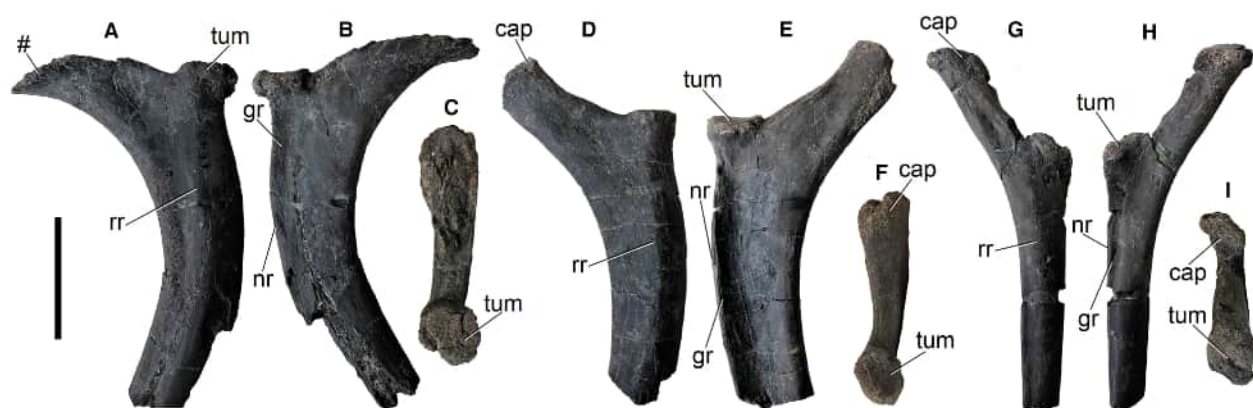


**FIG. 7.** *Istiorachis macarthurae* gen. et sp. nov. holotype (MIWG 6643). Three left dorsal rib heads. A–C, rib 1 in: A, anterior; B, posterior; C, dorsal view. D–F, rib 2 in: D, anterior; E, posterior; F, dorsal view. G–I, rib 3 in: G, anterior; H, posterior; I, dorsal view. Abbreviations: cap, capitulum; gr, groove; nr, narrow ridge; rr, rounded ridge; tum, tuberculum; #, fractured surface. Scale bar represents 50 mm.

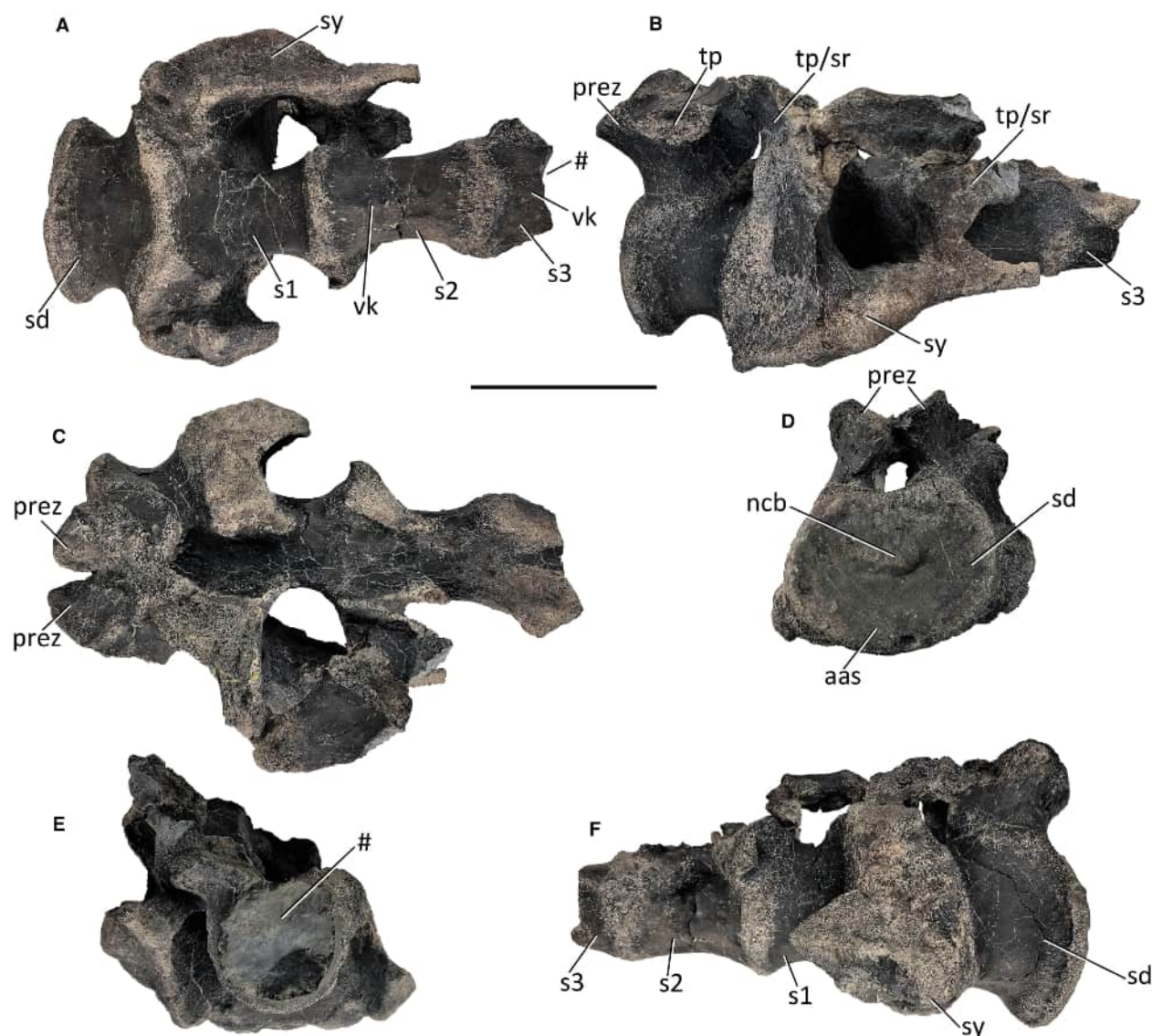


**FIG. 8.** *Istiorachis macarthurae* gen. et sp. nov. holotype (MIWG 6643). Anterior section of sacrum in: A, ventral; B, left lateral; C, dorsal; D, anterior; E, posterior; F, right lateral view. *Abbreviations:* aas, anterior articular surface; ncb, notochordal boss; prez, prezygapophysis; s, sacral vertebra; sd, sacrodorsal vertebra; sy, sacral yoke; tp, transverse process base; tp/sr, transverse process–sacral rib complex; vk, ventral keel; #, fracture surface. Scale bar represents 100 mm.

articular surface is essentially flat except for a centrally placed notochordal boss (Fig. 8D; ncb). The lateral walls of the centrum are flat dorsoventrally but deeply concave anteroposteriorly, giving the vertebra a spool-like shape in ventral view (Fig. 8A). The state of the neurocentral synchondrosis is difficult to judge due to abrasion. Posteriorly the centrum expands ventrally and transversely and is fused to the first sacral vertebra. The ventral surface of the sacrodorsal is smooth and almost flat with a nutrient foramen present on the left side but no evidence of a keel. A ventrally keeled sacrodorsal vertebra is present in *Cumnoria prestwichii* (Maidment *et al.* 2023),

*Barilium dawsoni* (Norman 2011) and on the anterior half of *Comptonatus chasei* but is absent from *Mantellisaurus atherfieldensis* (NHMUK PV R 5764), *Iguanodon bernisartensis* (Norman 1980) and *Morelladon beltrani* (Gasulla *et al.* 2015). The centrum is quite short longitudinally, being shorter than any of the preserved more anterior dorsal vertebrae. The neurapophyses supported transverse processes but only the fractured base on the left is present (Fig. 8B; tp), which has convex margins dorsally and ventrally, joining to form two angular vertices in lateral view. The prezygapophyses have dorsomedially facing facets set at an obtuse angle in anterior view.

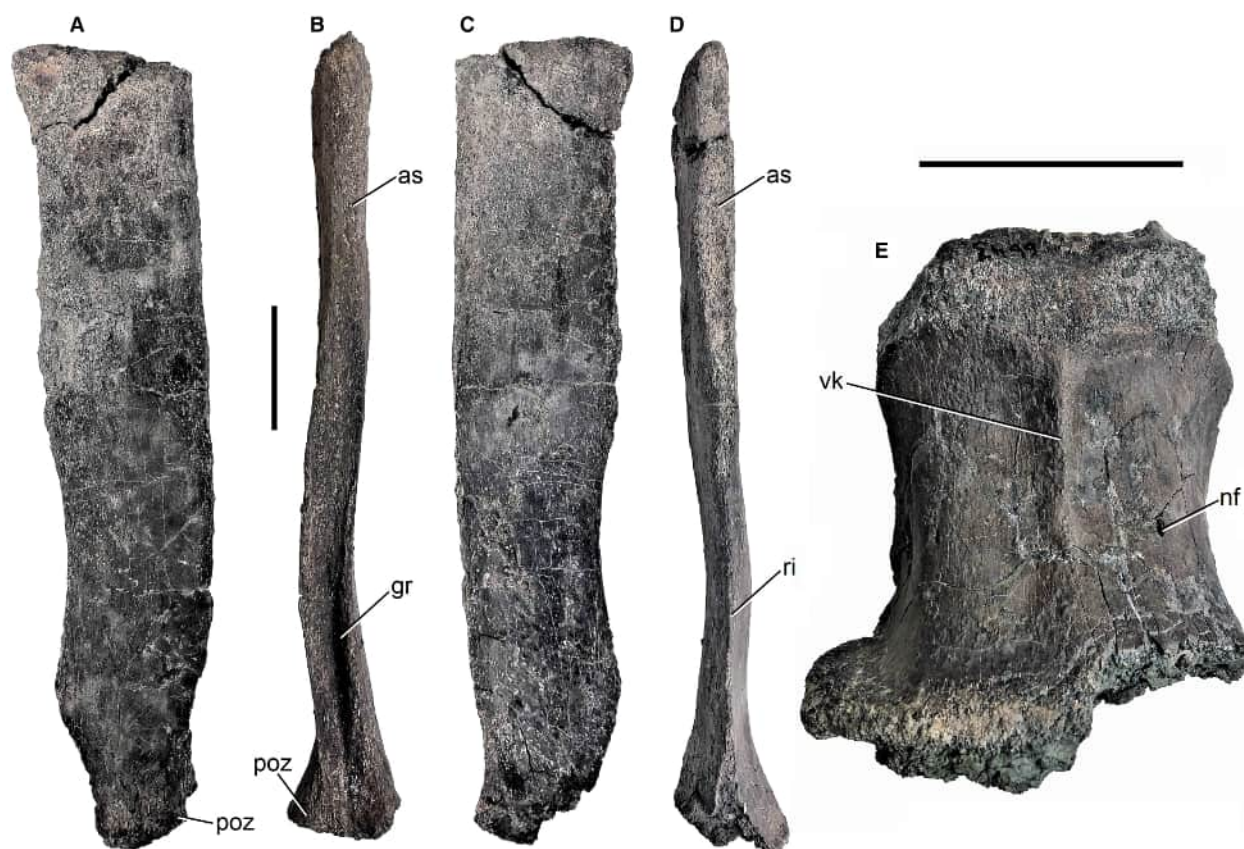


**FIG. 9.** *Istiorachis macarthurae* gen. et sp. nov. holotype (MIWG 6643). Sacral neural spine and ventral fragment of posterior sacral vertebra. A–D, neural spine in: A, left lateral; B, anterior; C, right lateral; D, posterior view. E, posterior sacral vertebra fragment in ventral view. Abbreviations: as, abraded surface; gr, groove; nf, nutrient foramen; poz, dorsal section of postzygapophysis; ri, ridge; vk, ventral keel. Scale bars represent 50 mm.

Posterior to the sacrodorsal, erosion of the neurapophyses reveals the neural canal, although some of the transverse process–sacral rib complexes are preserved (Fig. 8C). In ventral view, the anterior articular surface of the first true sacral vertebra is transversely expanded and fused to the sacrodorsal. There is no ventral keel present, the almost flat surface being smooth and very slightly concave transversely (Fig. 8A). The lateral walls of the centrum are dorsoventrally flat and concave anteroposteriorly, reducing the transverse width of the posterior articular surface to half that of the anterior surface (Fig. 8A). The second sacral has an obvious ventral keel (Fig. 8A; vk). The lateral walls of the centrum are less concave anteroposteriorly and there is little difference between the dimensions of the anterior and posterior articular surfaces. It is fused to the anterior section of the incomplete S3; the rest of this vertebra is unpreserved. A ventral keel is present on the small anterior section of the preserved ventral surface. The transverse process–sacral rib complexes are present bilaterally on S1 and on the left side of S2 but are badly damaged. The articular surface

for contact with the ilium is missing, but part of the sacral yoke is preserved (Fig. 8A–B, F; sy). A fragment preserving the ventral surface of another sacral vertebra was recovered, showing fusion at both ends (Fig. 9E). There is a strong longitudinal ventral keel (Fig. 9E; vk) separating two large, depressed areas on the ventral surface and some flaring is still evident at one end. This probably represents S4 or S5. The ventral surface of the sacrum in *Mantellisaurus atherfieldensis* is largely obscured by the armature, making interpretation difficult, but a ventral keel is probably present in S1 and S2 and absent in the more posterior vertebrae (Bonsor *et al.* 2023); *Brighstoneus simmondsi* has a keel on S1 but flat ventral surfaces on S2–S6, although S5 is damaged and the morphology less certain (Lockwood *et al.* 2021); *Morelladon beltrani* has a keel on S1, S2 and S4 (Gasulla *et al.* 2015).

An isolated but almost complete neural spine is preserved (Fig. 9A–D). The most dorsal parts of the postzygapophyses are attached at its base (Fig. 9A–B; poz), enabling its orientation to be determined. If complete, the sacral neural spine would probably have been slightly



taller dorsoventrally than the tall dorsal neural spine on D12 (see above). The anterior and posterior margins are damaged by abrasion in their dorsal half (although based on the elliptical shape of the dorsal surface of the neural spine, losses are minor), but in the ventral half, in lateral view, the anterior margin is gently concave and the posterior margin slightly convex but straighter, suggesting that the neural spine probably expanded slightly anteriorly as it extended dorsally (Fig. 9A, C). The ventral half also preserves a dorsoventrally orientated groove posteriorly, which expands transversely as it extends dorsally (Fig. 9B, gr). Anteriorly, the margin is blade-like ventrally and expands transversely as it extends dorsally. This suggests that adjacent spines slotted into each other. Contact between the sacral neural spines to form a continuous plate is seen in *Lesothosaurus diagnosticus* with some fusion present (Baron *et al.* 2017), *Hypsilophodon foxii* (Galton 1974), *Huehuecanauhtlus tiquichensis* (Ramírez-Velasco *et al.* 2012), *Iguanodon bernissartensis* (RBINS R51, RBINS R343, RBINS R341), RBINS R57 (Norman 1986), *Jinzhouosaurus yangi* (Wang *et al.* 2010), *Bactrosaurus johnsoni* (Godefroit *et al.* 1998) in which they are fused together, and *Tenontosaurus tilletti*, in which the

neural spines of large-bodied individuals contact each other and may start to fuse (Forster 1990), suggesting that ontogenetic variation may be present. In *Brighstoneus simmondsi* the spines also slot into one another, although the slot is on the anterior margin. The neural spines are separate in *Zalmoxes robustus* (Weishampel *et al.* 2003) and *Ouranosaurus nigeriensis* (Bertozzo *et al.* 2017).

### Caudal vertebrae

Seven caudal (Cd) vertebrae appear to form a sequence and are numbered Cd1–Cd7 (Fig. 10). Cd1 has features suggesting that it may have been the most posterior sacral or a sacrocaudal vertebra.

*Caudal vertebra 1 (sacrocaudal).* The neural spine is incomplete, and the right transverse process–rib complex is missing but the left is complete (Fig. 11). The anterior articular surface is transversely wider than dorsoventrally tall and was not fused to the rest of the synsacrum (Fig. 11A). However, its surface is atypically flat and apart from being marked by slight curved grooves extending



**FIG. 10.** *Istiorachis macarthurae* gen. et sp. nov. holotype (MIWG 6643). The anterior-most seven caudal vertebrae in left lateral view with neural spines reconstructed. Abbreviations: Cd, caudal vertebra; SC, sacrocaudal. Scale bar represents 50 mm.



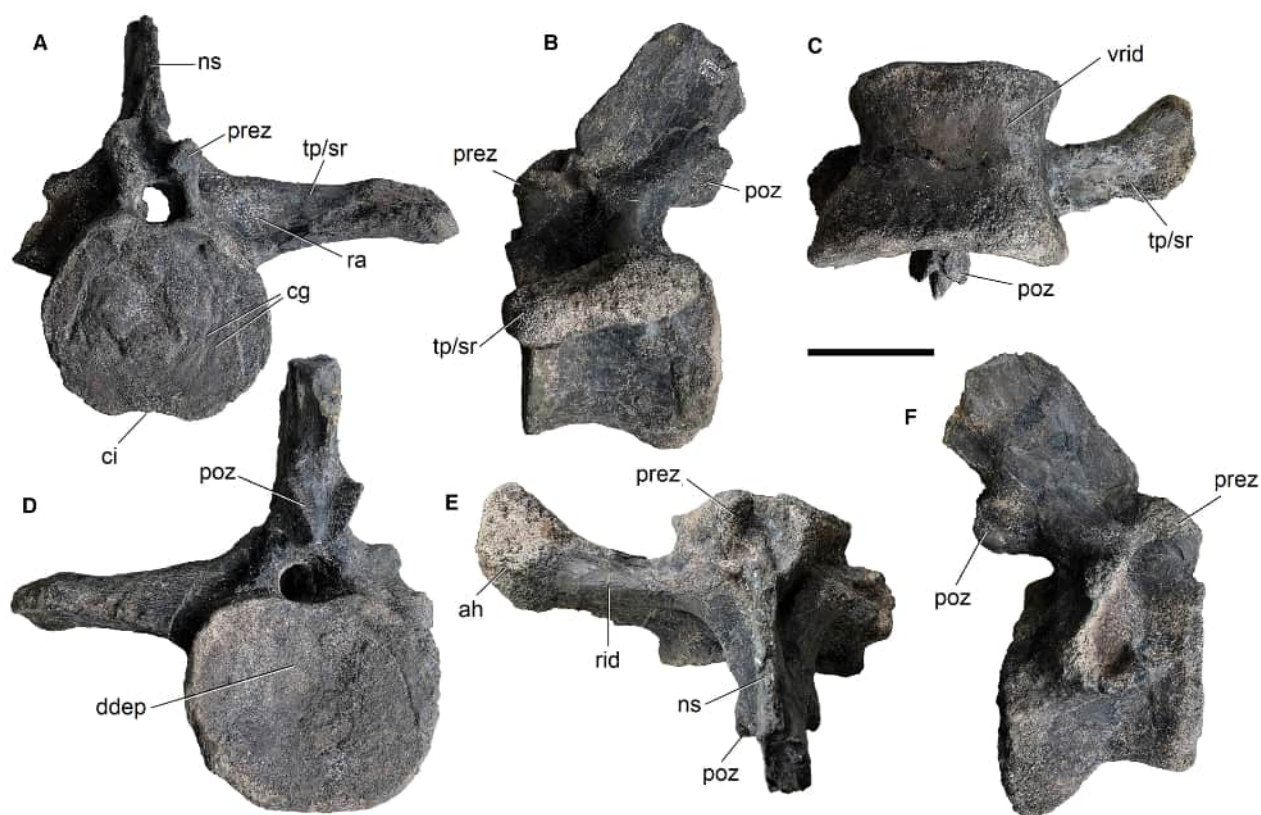


**FIG. 11.** *Istiorachis macarthurae* gen. et sp. nov. holotype (MIWG 6643). Sacrocaudal vertebra (Cd1) in: A, anterior; B, left lateral; C, ventral; D, posterior; E, dorsal; F, right lateral view. *Abbreviations:* ah, articular head; cg, curved grooves; ci, concave indentation; ddep, dorsal depressed area; ns, neural spine; poz, postzygapophysis; prez, prezygapophysis; ra, recessed area; rid, ridge; tp/sr, transverse process–sacral rib complex; vrid, ventral ridge. Scale bar represents 50 mm.

broadly parallel with the margin (Fig. 11A; cg), it is otherwise featureless, with little in the way of eversion of the margin. This might suggest that fusion of this articular surface with the sacrum was incipient. The posterior articular surface is wider transversely than dorsoventrally tall, both dimensions exceeding those of the anterior articular surface (Fig. 11D) and is situated more ventrally than the anterior surface (Fig. 11B, F), presumably to accommodate a descending tail. It has a concave depressed area in its dorsal half (Fig. 11D; dep) and the posterior margin is slightly everted. The lateral walls of the centrum are anteroposteriorly concave and dorsoventrally flat (Fig. 11B, F). There is no evidence of a neurocentral synchondrosis. The ventral surface of the centrum is flat with no keel or haemal facets (Fig. 11C), although ridges extend longitudinally along the lateral margins and bound a shallow, transversely concave depression that becomes more prominent anteriorly and forms a concave indentation on the ventral margin of the anterior articular surface (Fig. 11A; ci). This creates what might be termed a very shallow, broad ventral sulcus. The neuropophyses and transverse process and rib are situated dorsally at the

midpoint of the centrum rather than being shifted anteriorly as in typical sacral vertebrae (Norman 1980). However, these characteristics can also be observed in the most posterior sacral centrum of some specimens of *Iguanodon bernissartensis* (Norman 1980, fig. 45). This is in part a nomenclatural problem, with some authors using the term ‘true’ sacral vertebra for all vertebrae that contact the ilium, and sacrocaudal or sacrodorsal for those that are part of the synsacrum but have free-standing transverse processes and ribs (e.g. Galton 2012), while others regard ‘true’ sacral vertebrae as those that are homologous with the primordial sacral vertebrae that were plesiomorphic for Ornithischia, and refer to subsequent additions as sacrocaudals or sacrodorsals, regardless of contact with the ilium (e.g. Carpenter & Wilson 2008). The pre- and postzygapophyseal facets are steeply inclined with an acute angle between them (Fig. 11A, D). The facets of the postzygapophyses face ventrolaterally and the prezygapophyses dorsomedially. The transverse process–rib complex is a robust structure. Proximally there is a strong, laterally extending, anteroposteriorly convex dorsal ridge (Fig. 11E; rid), giving it a

subtriangular cross-section with a flat ventral surface, and posterodorsally and anterodorsally facing surfaces. A recessed area is present on the anterodorsal surface, ventral to the ridge (Fig. 11A; ra). The appearance suggests that the ridge is the transverse process, fused to a rib in similar fashion to that seen in some sacral vertebrae, such as *Iguanodon bernissartensis* (Norman 1980, Gasulla *et al.* 2022), *Morelladon beltrani* (Gasulla *et al.* 2015) and *Comptonatus chasei* (Lockwood *et al.* 2024). In typical caudal vertebrae of extant reptiles, including crocodilians, the transverse process is usually fused indistinguishably with the caudal rib during embryonic development (e.g. Rieppel 1993, 1994; Persons & Currie 2011). As the process extends laterally, it becomes slightly dorsoventrally compressed and more elliptical in cross-section before expanding, predominantly anteriorly but also slightly posteriorly, to form a large convex distal surface, suggesting articulation (but not fusion) with the ilium or sacral yoke. The angle of the neural spine is directed posterodorsally at *c.* 45°, similar to the other caudal vertebrae (see below), whereas sacral neural spines in iguanodontians, especially those more anteriorly placed, tend to be upright (Norman 1980). Sections of the caudal neural spine, when reconstructed (Fig. 10), suggest it was hyperelongate and perhaps *c.* fourfold the dorsoventral height of the anterior articular surface.

**Caudal vertebrae 2–7.** Extending posteriorly, the anterior caudal vertebrae retain similar anteroposterior lengths, but the dorsoventral height and transverse width both decrease, the latter more so, so that the vertebrae become both gradually smaller and more transversely compressed (Figs 10, 12). In Cd2–3 the transverse width of both articular surfaces is greater than the dorsoventral height, but in Cd4–7 the height is greater than the width (Fig. 12).

The articular surfaces are rounded in outline in Cd2, heart shaped in Cd3 and oval (long axis dorsoventral) but tapering slightly ventrally in Cd4–7. The dorsal half of the anterior articular surface of Cd2 protrudes slightly (Fig. 12A; dpro), so that in lateral view the dorsal margin extends further anteriorly than the ventral margin and would have articulated with the dorsal recess in the posterior articular surface of Cd1. A similar bulge is described on the anterior articular surface of the first caudal vertebra of RBINS R57 (Norman 1986), which articulated with a corresponding recess in the posterior articular facet of the last sacral vertebra (Norman 1986). This character is also found in *Iguanodon bernissartensis* (Norman 1980) and *Brighstoneus simmondsi* (Lockwood *et al.* 2021). The posterior articular surface of Cd2 also has a dorsal recess (Fig. 12B; ddep), which articulates with a dorsal bulge in the anterior articular surface of Cd3. The same character is seen between Cd3 and Cd4

but is less marked and thereafter is not evident. As in Cd1, the posterior articular surface of Cd2 is set ventrally to the anterior articular surface. This is not apparent in subsequent vertebrae. Cd2 and Cd3 have a notochordal boss (Fig. 12B, I; nb) located at the centre of the posterior articular surface.

Cd2 has no haemal facets (Fig. 12D), Cd 3 has a posterior facet (Fig. 12G; phf) and thereafter each centrum has anterior and posterior facets (Fig. 12O; ahf, phf). Among non-hadrosaurid iguanodontians, the first chevron facet appears posteriorly on Cd3 in *Ouranosaurus nigeriensis* (Taquet 1976; Bertozzo *et al.* 2017), and probably in *Probaetosauros gobiensis* (Norman 2002), *Jinzhousaurus yangi* (Wang *et al.* 2010) and *Comptonatus chasei* (Lockwood *et al.* 2024), which also have two disarticulated caudal vertebrae without obvious haemal facets. In hadrosaurids the first chevron is posterior to Cd4 or Cd5 in saurolophines, and on Cd2 or Cd3 in lambeosaurines (Horner *et al.* 2004), but in most other iguanodontians in which the character is preserved, the first chevron facet is sited posteriorly on Cd2: such as *Valdosaurus canaliculatus* (Barrett 2016), *Dysalotosaurus lettowvorbecki* (Janensch 1955), *Uteodon aphanoecetes* (Carpenter & Wilson 2008), possibly *Cumnoria prestwichii* (Maidment *et al.* 2023), *Tenontosaurus tilletti* (Forster 1990), *Camptosaurus dispar* (Gilmore 1909), *Iguanodon bernissartensis* (Norman 1980), RBINS R57 (Norman 1986), *Bolong yixianensis* (Wu & Godefroit 2012), *Barilium dawsoni* (Norman 2011), *Gobihadros mongoliensis* (Tsogtbaatar *et al.* 2019) and *Brighstoneus simmondsi* (Lockwood *et al.* 2021). In ventral view the anterior haemal facets are D shaped with the curve facing posteriorly, while the posterior facets are B shaped with the curves facing anteriorly (Fig. 12O).

Cd2 has a flat ventral surface, while Cd3–7 have a longitudinal ventral sulcus between two longitudinal parasagittally placed ridges. Sulci are present in the proximal caudal vertebrae in some fragmentary examples of *Zalmoxes robustus* (Weishampel *et al.* 2003), *Valdosaurus canaliculatus* (Barrett 2016), *Magnamanus soriaensis* (Fuentes Vidarte *et al.* 2016), *Brighstoneus simmondsi* (Lockwood *et al.* 2021) and *Comptonatus chasei* (Lockwood *et al.* 2024). Cd2 has nine small nutrient foramina on its ventral surface (Fig. 12D; nf) as well as one on the left lateral surface of the centrum.

The lateral walls of the centrum are dorsoventrally straight and anteroposteriorly concave, so are gently spool shaped in ventral view. There are no definite open neurocentral synchondroses visible and the caudal ribs all appear solidly fused.

In Cd2 only the fractured bases of the caudal ribs remain (Fig. 12E), and these are large and subtriangular with the apex pointing dorsally. In subsequent vertebrae the caudal rib is a dorsoventrally compressed blade with a

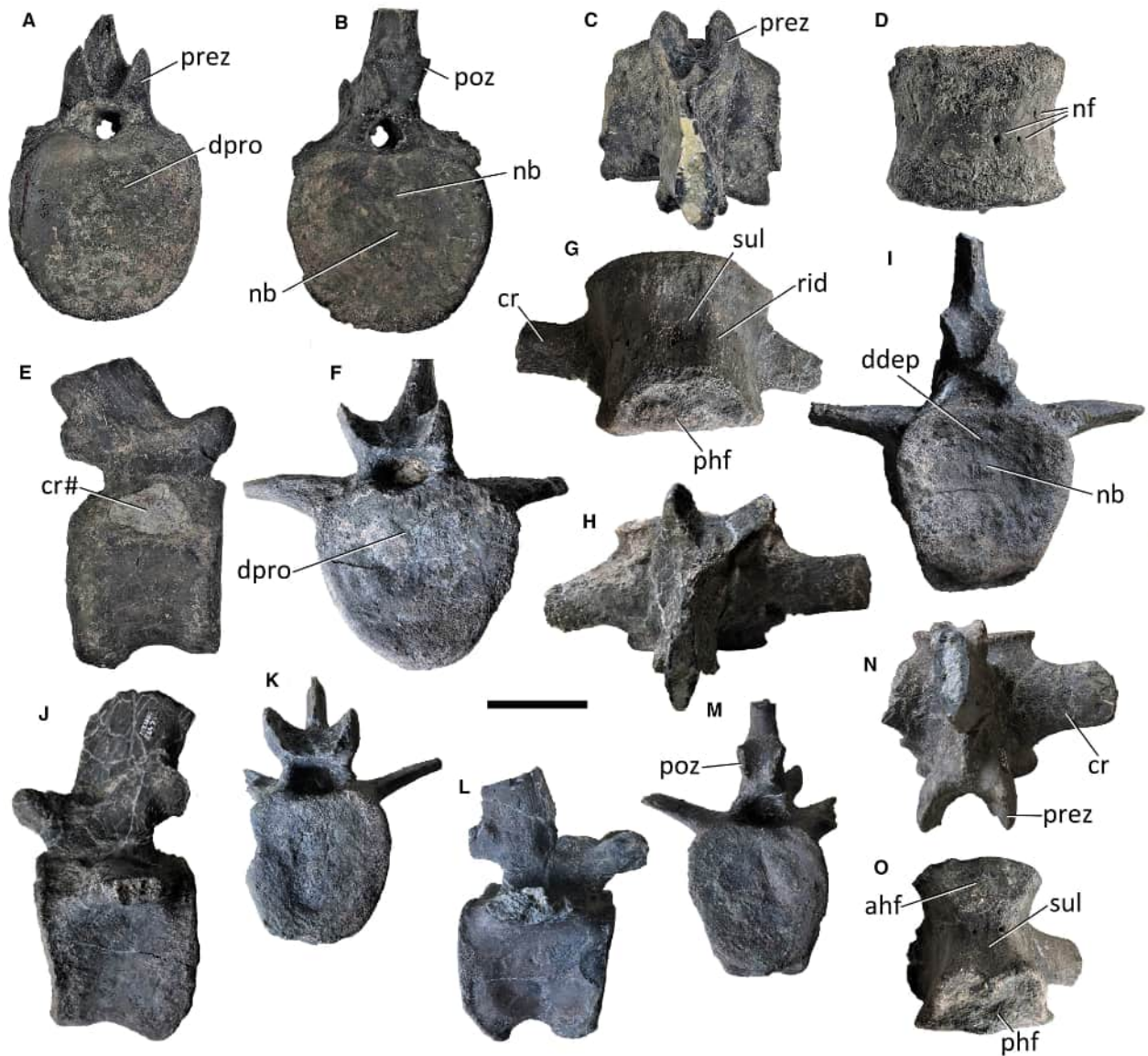


**FIG. 12.** *Istiorachis macarthurae* gen. et sp. nov. holotype (MIWG 6643). Caudal vertebrae Cd2, Cd3 and Cd7. A–E, Cd2 in: A, anterior; B, posterior; C, dorsal; D, ventral; E, right lateral view. F–J, Cd3 in: F, anterior; G, ventral; H, dorsal; I, posterior; J, left lateral view. K–O, Cd7 in: K, anterior; L, right lateral; M, posterior; N, dorsal; O, ventral view. *Abbreviations:* ahf, anterior haemal facet; cr, caudal rib; ddep, dorsal depression; dpro, dorsal protrusion; nb, notochordal boss; nf, nutrient foramina; phf, posterior haemal facet; poz, postzygapophysis; prez, prezygapophysis; rid, ridge; sul, sulcus; #, fracture surface. Scale bar represents 50 mm.

flattened elliptical cross-section. In anterior view (Fig. 12F, J), the rib has a straight to mildly convex dorsal margin and gently concave ventral margin so that the blade becomes thinner as it extends laterally or slightly dorsolaterally in the more posterior vertebrae. In dorsal view (Fig. 12H, N) the rib is rectangular (long axis transverse) and extends slightly posterolaterally.

In all caudal vertebrae the prezygapophyses are steeply inclined with dorsomedially facing articular facets, matching the ventrolaterally facing facets on the

postzygapophyses (Fig. 12; prez, poz). The space between the prezygapophyseal facets in Cd2 is relatively narrow and the postzygapophyseal facets of the preceding vertebrae would have fitted quite tightly (Fig. 12A). This is not the case in Cd3–7 where, although the prezygapophyseal facets are still steeply inclined, they are widely separated (Fig. 12F, K) and, although the facets face dorsomedially in anterior view, in dorsal view they also face antero-medially and are connected to each other by an anteriorly concave, smooth surface (Fig. 12H, N). The space



between the prezygapophyseal facets is wider than the maximum width of the postzygapophyses by up to 48%, presumably indicating a large cartilaginous component.

The neural spines are complete only in Cd5–7, although fragments enable a possible reconstruction (Fig. 10). In lateral view the spines extend postero-dorsally, with almost straight margins, which are very slightly concave anteriorly. The anteroposterior diameter of the neural spines is relatively narrow compared with the dorsal and sacral vertebrae but is slightly expanded distally. The base of the neural spine in Cd2 has a dorso-ventrally orientated groove anteriorly and a ridge posteriorly, the latter ending just dorsal to the postzygapophyses. This suggests that the neural spine may have contacted the adjacent neural spines, at least ventrally. Moving posteriorly along the series, the neural spines decrease in dorsoventral height both in relative and absolute terms.

### *Pubes*

Both pubes are preserved and show little evidence of distortion, but both are missing the anterior part of the prepubic blade and the distal section of the postpubic rod to similar degrees (Fig. 13).

Posteriorly, the pubis consists of a robust and transversely compressed body. The posterior surface of the body is concave in lateral view (Fig. 13C), transversely flat and provides the pubic contribution to the acetabulum. The acetabular surface faces posterolaterally and has an everted lateral margin (Fig. 13C). As it extends dorsally, the acetabular surface expands transversely and forms the posterior surface of the iliac process. This stout process projects posterodorsally to support a sub-triangular, slightly domed and rugose dorsal surface for articulation with the pubic peduncle of the ilium (Fig. 13; ilp). The apex of the triangle extends anteriorly to continue as the dorsal margin of the prepubic process. Ventrally, the acetabular surface provides the posterolateral surface of the smaller ischial process (Fig. 13; isp). Anteriorly, the ischial process forms the posterior margin of the oval (long axis dorsoventral) obturator foramen (Fig. 13; obf), but distally it curves anteriorly to contribute to the posteroventral margin of the foramen. The anterior margin of the obturator foramen is provided by the base of the postpubic rod (Fig. 13; ppr), from which a small process extends posteriorly to provide the anteroventral margin of the foramen. In both specimens this process is damaged slightly but does not contact the ischial process. The postpubic rod is incomplete but its proximal section is subtriangular in cross-section with lateral, anteromedial and posteromedial surfaces. The postpubic rod extends posteroventrally in lateral view (Fig. 13C) and in

posterior view is angled slightly medially to the long axis of the acetabular surface (Fig. 13B). Anteriorly the base of the postpubic rod continues as the ventral margin of the prepubic process.

The neck and commencement of the distal dorsoventral expansion of the prepubic process is preserved in both specimens. The dorsal margin is quite robust (transverse width 35 mm in its proximal section) and in dorsal view it is transversely convex, gradually becoming thinner and curving gently laterally as it extends anteriorly. In lateral view it is slightly concave proximally but distally it becomes increasingly concave as the prepubic process expands dorsally (Fig. 13C). The ventral margin is much more delicate and blade-like, with a transverse diameter of c. 3 mm. In ventral view it is straight proximally but extends sinusoidally, curving medially then laterally, and slightly warping the surface of the prepubic process. In lateral view it is almost straight. The shape of the neck suggests that the dorsoventral expansion of the distal section of the prepubic blade was relatively pronounced and predominantly dorsally orientated, as in *Mantellisaurus atherfieldensis* (NHMUK PV R 5764), RBINS R57 and *Hypselospinus* cf. *fittoni* (NHMUK PV R 811), but unlike *Iguanodon bernissartensis* (RBINS R51), which has a longer neck and is then expanded dorsally and ventrally, and *Comptonatus chasei*, which has a similar neck length to *Istiorachis macarthurae* but is markedly expanded dorsally and ventrally (Lockwood *et al.* 2024).

### *Ischia*

Both ischia are preserved (Fig. 14). They are described with the long axis of the shaft orientated dorsoventrally.

The proximal end of the ischium is transversely compressed and divided into two processes (Fig. 14). The iliac peduncle (Figs 14, 15B; ilp) extends posterodorsally and is considerably larger and more robust than the pubic peduncle (Figs 14, 15A–B; pup), which extends antero-dorsally. The margins of the iliac peduncle are almost parallel and unlike *Brighstoneus simmondsi* (MIWG 6344) and *Comptonatus chasei* (IWCMS 2014.80) hardly flare as they extend towards the articular surface. The articular surface is rugose, with the rugosity extending onto the dorsal margin of the shaft of the peduncle, represented by dorsoventrally orientated striae. The articular surface faces predominantly dorsally but is tilted slightly postero-dorsally and is anteroposteriorly elongate, with a rounded posterior margin and a more pointed anterior margin. The posterodorsal section of the surface extends posteriorly so that it overhangs the peduncle in lateral view (Fig. 15A; pex). This feature is well-developed in lambeosaurines (Wagner 2001; Brett-Surman & Wagner 2007), but is also seen in some non-hadrosaurid iguanodontians



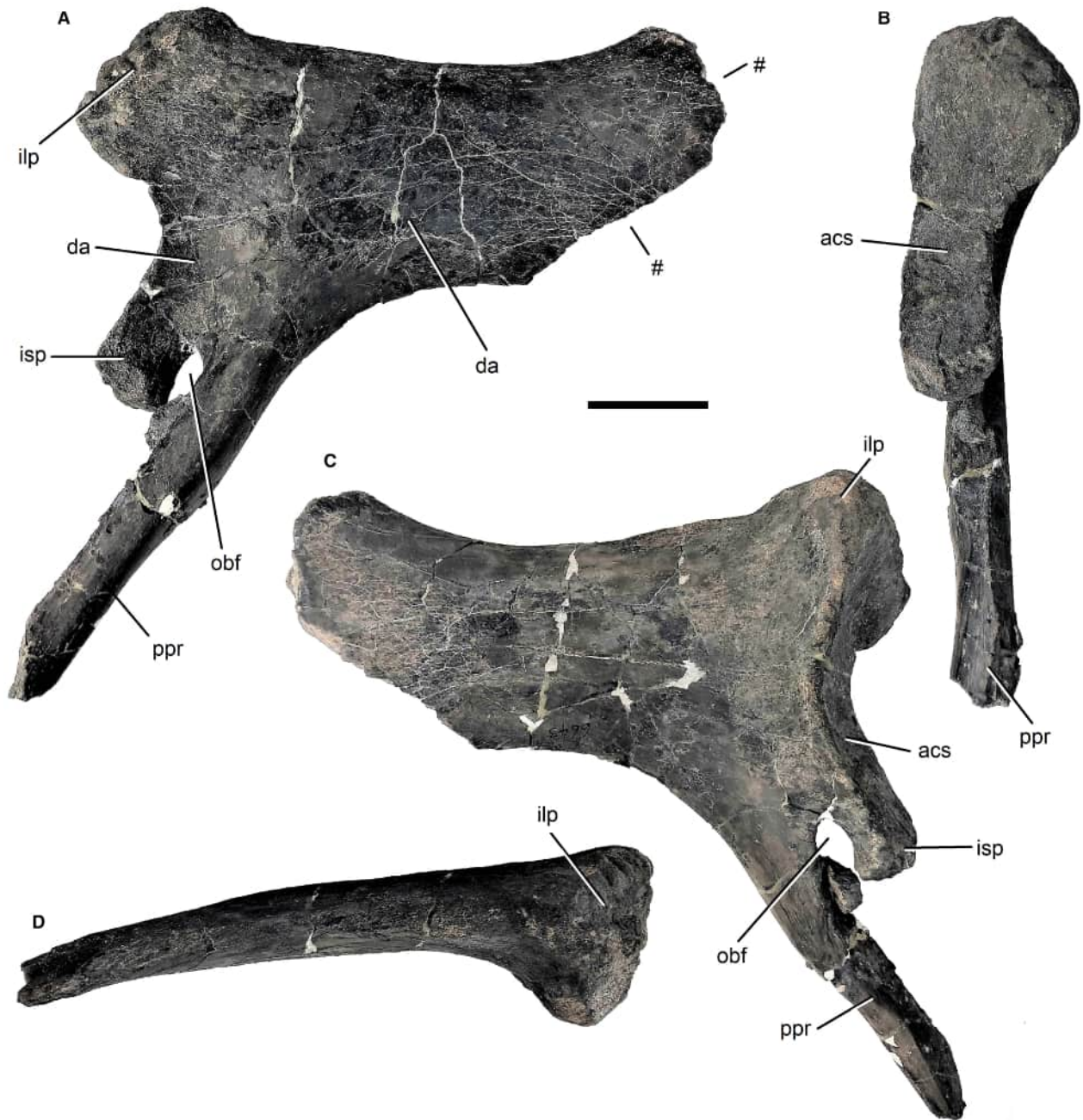


**FIG. 13.** *Istiorachis macarthurae* gen. et sp. nov. holotype (MIWG 6643). Left pubis in: A, medial; B, posterior; C, lateral; D, dorsal view. Abbreviations: acs, acetabular surface; da, depressed area; ilp, iliac process; isp, ischial process; obf, obturator foramen; ppr, post-pubic rod; #, fracture surface. Scale bar represents 50 mm.

such as *Tenontosaurus tilletti* (Ostrom 1970), *Cumnoria prestwichii* (Maidment et al. 2023), *Delapparentia turolensis* MPZ 2014/328 (Gasca et al. 2014), *Morelladon beltrani* (Gasulla et al. 2015), *Eolambia caroljonesa* (McDonald et al. 2012) and *Gilmoresaurus mongoliensis* (Prieto-Márquez & Norrell 2010). In lateral view a transversely thin concave ridge of bone extends from the

pointed anterior end of the iliac peduncle to the pubic peduncle (Fig. 14A, C). The lateral surface below this curved margin provides the ischial contribution to the acetabulum (Figs 14A, C, 15B; ace). Anteriorly, the pubic peduncle has a smaller and less rugose anterodorsally facing, triangular articular surface, with the apex directed anteroventrally. This differs from the articular surface of



**FIG. 14.** *Istiorachis macarthurae* gen. et sp. nov. holotype (MIWG 6643). Both ischia. A–B, left ischium in: A, lateral; B, medial view. C–D, right ischium in: C, lateral; D, medial view. Abbreviations: ace, acetabulum; cr#, crush fracture; ilp, iliac peduncle; isb, ischial boot; lar, lateral ridge; mer, medial ridge; pup, pubic peduncle; sh, shaft; #, fracture surface. Scale bar represents 100 mm.

*Comptonatus chasei*, which has anterodorsal and antero-ventral facing facets (Lockwood *et al.* 2024). In lateral view the ventral margin of the pubic peduncle extends posteroventrally as a thin ridge of bone. Initially this is straight (but this area is a fracture surface on both ischia) before curving concavely and forming the dorsal half of the ischiopubic foramen (*sensu* Lockwood *et al.* 2024). The ventral part of this foramen would have been formed by the obturator process, but this has not been preserved in either specimen. It is possible that the fractured surface on the ventral margin of the pubic process originally extended ventrally to give the ischiopubic foramen a bony

anterodorsal margin, as seen in *Bactrosaurus johnsoni* (Godefroit *et al.* 1998) and some hadrosaurids such as in *Eotrachodon orientalis* (Prieto-Márquez *et al.* 2016), *Brachylophosaurus canadensis* (Prieto-Márquez 2001) and *Saurolophus osborni* (Brown 1913b).

In lateral view the ischial shaft is essentially straight in its dorsal half, although slightly convex anteriorly. As it extends ventrally, the posterior margin becomes convex and the anterior margin concave, the concavity becoming more prominent distally as it approaches the ischial boot. Overall, this gives the shaft a somewhat sinusoidal shape. In the left ischium there is a crushed and fractured area



**FIG. 15.** *Istiorachis macarthurae* gen. et sp. nov. holotype (MIWG 6643). Left ischium. A–B, close up of proximal section in: A, medial; B, lateral view. C–E, close up of distal section in: C, lateral; D, medial; E, ventral view. *Abbreviations:* ace, acetabulum; ant, anterior; cru#, crush fracture; ilp, iliac peduncle; isb, ischial boot; lar, lateral ridge; pex, posterior extension; pos, posterior; pup, pubic peduncle; #, fracture surface. Scale bars represent 50 mm.

posteriorly just dorsal to the boot, and the boot has separated from the shaft. However, the boot fits perfectly in its anterior section and the crushing does not appear to have distorted the morphology of the anterior margin. A sinusoidal shaft of the ischium is seen in *Bactrosaurus johnsoni* (Gilmore 1933) and *Gilmoresaurus mongoliensis* (Prieto-Márquez & Norrell 2010). More generally the shafts of iguanodontian ischia fall between being straight, as in *Uteodon aphanocetes* (Carpenter & Wilson 2008), *Altirhinus kurzanovi* (Norman 1998), *Morelladon beltrani* (Gasulla et al. 2015) and *Choyrodon barsboldi* (Gates

et al. 2018), and concavely curved anteriorly, as in *Zalmoxes robustus* (Weishampel et al. 2003), *Camptosaurus dispar* (Carpenter & Wilson 2008), *Hypselospinus fittoni* (Norman 2015) and *Iguanodon bernissartensis* (RBINS R51). There is some evidence of intraspecific variation in this character, with the shaft varying between straight and ventrally kinked in its lower third in *Tenontosaurus tilletti* (Forster 1990), and usually anteriorly concave but with some straight examples in *Iguanodon bernissartensis* (Verdú et al. 2017), although the latter may be due to distortion. No ontogenetic variation was recorded in the



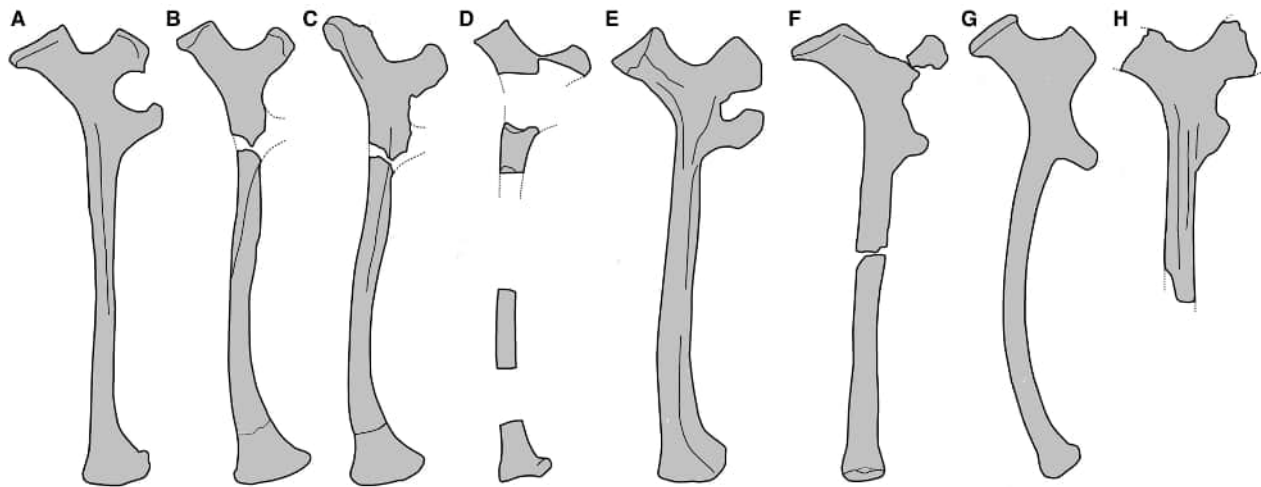


**FIG. 16.** Ischia of selected iguanodontians in lateral view unless otherwise stated. A, *Comptonatus chasei* (after Lockwood *et al.* 2024). B, *Istiorachis macarthurae* (medial). C, *Istiorachis macarthurae*. D, *Mantellisaurus atherfieldensis* (after Hooley 1925). E, *Ouranosaurus nigeriensis* (after Taquet 1976). F, *Morelladon beltrani* (after Gasulla *et al.* 2015). G, *Iguanodon bernissartensis* (after Norman 1986). H, *Brighstoneus simmondsi* (after Lockwood *et al.* 2021). All scaled to approximately the same length.

morphology of the ischial shaft of *Bactrosaurus johnsoni* and *Gilmoresaurus mongoliensis* by Brett-Surman & Wagner (2007). The proximal shaft is sub-triangular in cross-section, the apex forming a lateral ridge (Figs 14A, 15B; lar). This differs from the proximal section of the lateral surface of the shaft in *Brighstoneus simmondsi*, which is deeply dorsoventrally grooved (Lockwood *et al.* 2021). The lateral ridge in *Istiorachis macarthurae* extends down the shaft from the midpoint of the proximal shaft, gradually migrating anteriorly to become the anterior margin of the shaft. In medial view, a ridge (Fig. 14B; mer) commences proximally on the anterior margin (where it would have been an extension of the ventral margin of the obturator process) and extends diagonally across the shaft to become the posterior margin. The combination of these ridges gives the shaft a twisted appearance.

Distally, the ischium expands predominantly anteriorly and is transversely compressed to form the ischial boot (Figs 14, 15C–D; isb). The maximum anteroposterior measurement of the boot is 137 mm, which is 3.3-fold the maximum midshaft diameter and 55% of the maximum diameter of the proximal ischium in lateral view. This is much more developed than in *Iguanodon bernissartensis* (Verdú *et al.* 2017), *Mantellisaurus atherfieldensis* (NHMUK PV R 5764), in which the boot is preserved although damaged and described by Norman (1998) as ‘slightly booted’, and *Morelladon beltrani*, in which there is only a slight anteroposterior and transverse expansion (Gasulla *et al.* 2015). A small ischium (NHMUK PV R 11521) from the Isle of Wight referred to *Mantellisaurus*

*atherfieldensis* (Barrett *et al.* 2009b; McDonald 2012a; Norman 2012) is also straight and weakly booted.

The ischial boot is not preserved in many iguanodontian taxa but a boot to shaft ratio of 3.3 is greater than in any other Wealden Group specimen, and rivals that of any other non-hadrosaurid iguanodontian, although the ischia of *Bactrosaurus johnsoni* (Gilmore 1933, fig. 38) and *Eolambia caroljonesa* (McDonald *et al.* 2012) are similar. Although there is evidence that the ischial boot develops during ontogeny in *Gilmoresaurus mongoliensis* (Brett-Surman & Wagner 2007) and *Hypacrosaurus stebingeri* (Guenther 2007), *Istiorachis macarthurae* and *Mantellisaurus atherfieldensis* are similar-sized animals and both have visible neurocentral synchondroses and yet very different distal ischia (Fig. 16B–D). *Istiorachis chasei* also lacks the widely flared distal iliac peduncle and double-faceted pubic peduncle of *Comptonatus chasei* and the deep lateral groove in the proximal shaft of *Brighstoneus simmondsi* (Fig. 16H).

## RESULTS

### Phylogeny

The equally weighted phylogenetic analysis (Fig. 17A) resulted in 45 MPTs, with tree lengths of 357 steps. The consistency index is 0.560, the rescaled consistency index is 0.483 and the retention index is 0.863.

A strict consensus tree produced from these MPTs showed no significant differences from the results obtained



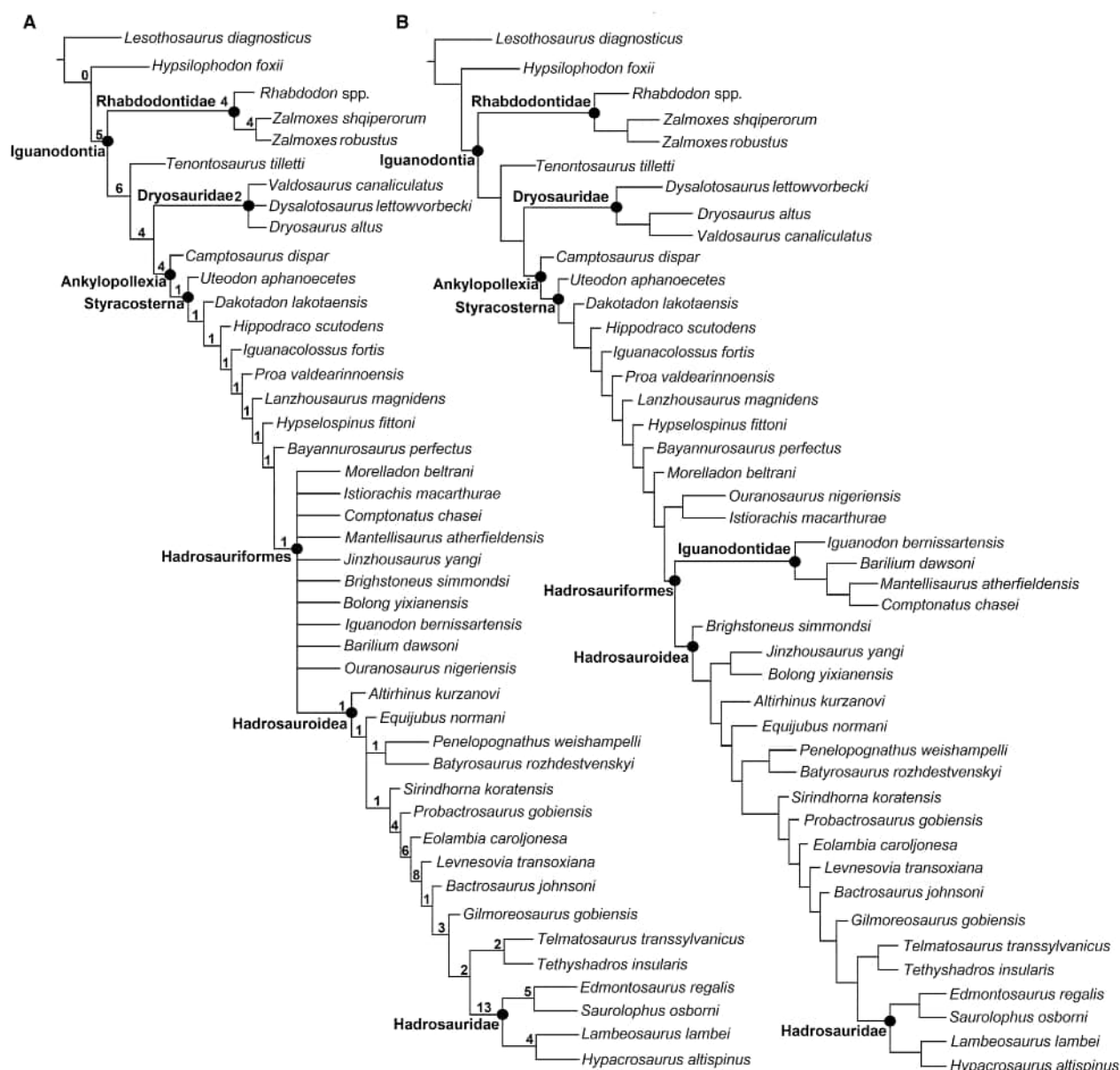


**FIG. 17.** Cladograms of the phylogenetic relationships of *Istiorachis macarthurae*. A, strict consensus of 45 retained trees; tree length = 357 steps, consistency index = 0.560, rescaled consistency index = 0.483, retention index = 0.863; Bremer support indices are given above the line (TNT bootstrap values are shown in Appendix S1; Fig. S27). B, cladogram of the tree in A but with extended implied weighting ( $k = 3$ ).

by Xu *et al.* (2018) regarding the relationships between the major clades nested within Iguanodontia: Rhabdodontidae, Dryosauridae, Ankylopollexia, Styrcosterna, Hadrosauriformes and Hadrosauridae. However, *contra* Xu *et al.* (2018), the potentially monophyletic clade Iguanodontidae (Godefroit *et al.* 2012; Norman 2015) was not recovered. *Istiorachis macarthurae* was recovered in a polytomy at the base of Hadrosauriformes with the other Wessex Formation taxa *Brighstoneus simmondsi*, *Iguanodon bernissartensis*, *Mantellisaurus atherfieldensis* and *Comptonatus chasei*,

along with *Ouranosaurus nigeriensis*, *Morelladon beltrani*, *Jinzhousaurus yangi* and *Bolong yixianensis*. Dryosauridae was also recovered as a polytomy including *Dryosaurus altus*, *Dysalotosaurus lettowvorbecki* and *Valdosaurus canaliculatus*. Support for these relationships is extremely weak with Bremer indices of 1 and bootstrap values below or just above 50%, and thus caution in their interpretation is needed.

To further explore the causes of instability within the polytomy, an analysis with extended implied weighting

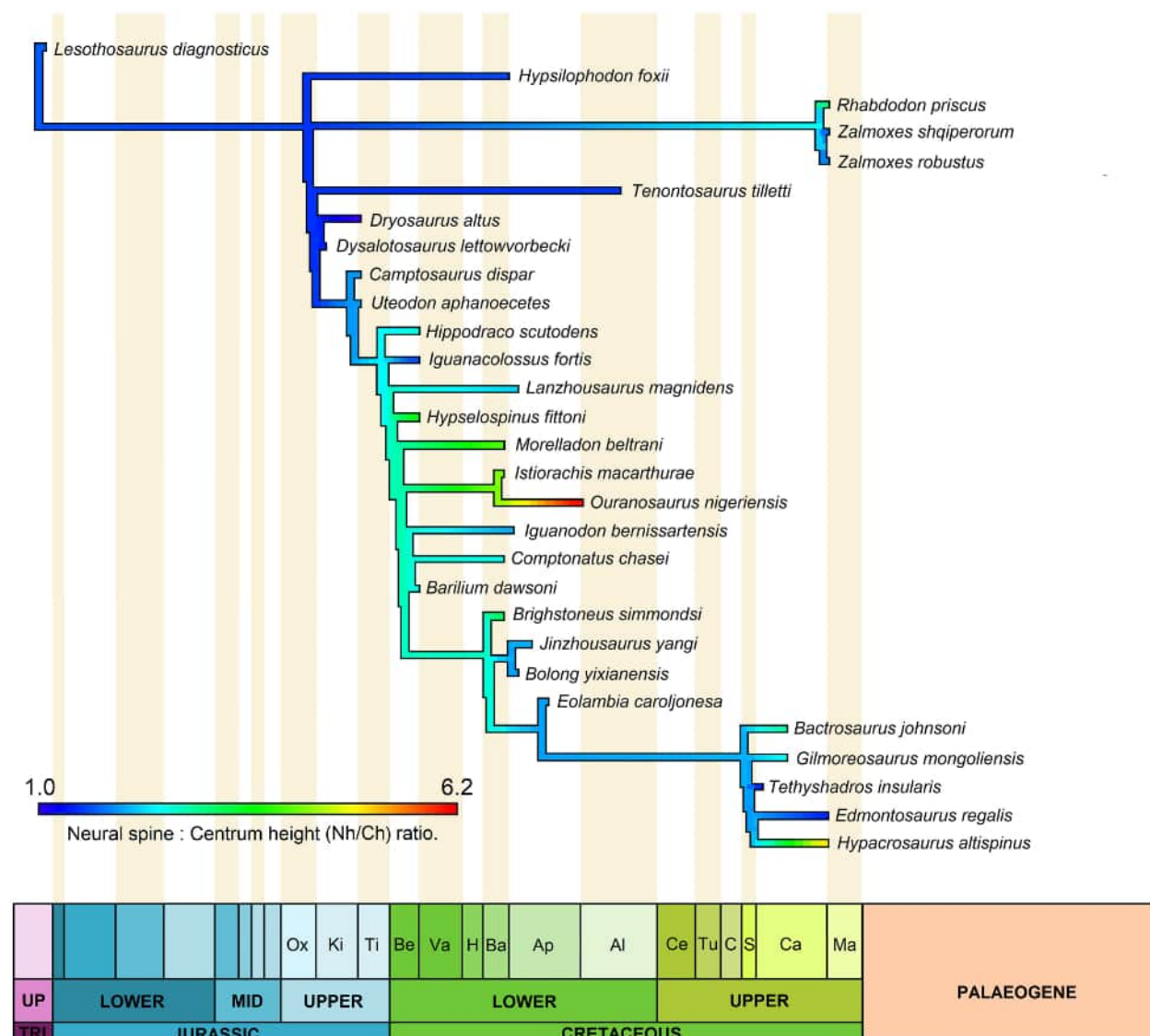


**FIG. 18.** Time-calibrated heat map of ancestral state reconstruction for iguanodontian neural spine height to centrum height ratios (Nh/Ch) in posterior dorsal vertebrae. Extended implied weighting ( $k = 3$ ) tree with pruning of taxa lacking data. Minimum branch length set to 0.5 Ma. Geological stages: Al, Albian; Ap, Aptian; Ba, Barremian; Be, Berriasian; C, Coniacian; Ca, Campanian; Ce, Cenomanian; H, Hauterivian; Ki, Kimmeridgian; Ma, Maastrichtian; Ox, Oxfordian; S, Santonian; Ti, Tithonian; Tu, Turonian. See Appendix S1 for nodal values of Nh/Ch.

( $k = 3$ ) was carried out. A single MPT was recovered, in which *Istiorachis* was recovered as the sister taxon of *Ouranosaurus* (Fig. 17B).

#### Neural spines of iguanodontian dorsal vertebrae

The results of the ancestral states reconstruction (Fig. 18) show that in iguanodontians the relative height of the neural spines on the posterior dorsal vertebrae began to increase at the Jurassic–Cretaceous boundary, with the

heat map demonstrating the establishment of elongation during the Berriasian. The ancestral nodes (Appendix S1; Fig. S31; Table S7) indicate that low neural spines were present in early-diverging ornithomorphs and iguanodontians, with little change occurring until the ancestral node for Ankylopollexia (the least inclusive clade containing *Camptosaurus dispar* and *Parasaurolophus walkeri* (Sereno 1986); see Fig. 17 for clade names). Ancestral values for neural spine length increased somewhat at this point but never to the degree seen in *Ouranosaurus nigeriensis* or *Istiorachis macarthurae*. After the generalized neural

spine elongation observed in the Berriasian the time-calibrated heat map shows continued elongation in some branches and apparent reversion to a more plesiomorphic state in others. Continued elongation of the neural spines is seen in the branches to *Hypselospinus fittoni*, *Morelladon beltrani* and the sister taxa *Istiorachis macarthurae* and *Ouranosaurus nigeriensis*. Branches such as those to *Iguanacolossus fortis*, *Bolong yixianensis*, *Iguanodon bernisartensis* and *Jinzhouosaurus yangi* appear to have autapomorphically reverted back to the plesiomorphic state. The result is a wide range of relative neural spine heights throughout the Early Cretaceous (Fig. 18). Although taxon sampling is poor in this part of the tree, there appears to have been a synapomorphic reversal to lower neural spines within Hadrosauroidea, before several taxa independently elongated their neural spines in the Late Cretaceous (Fig. 18).

*Rhabdodon priscus* shows a considerable degree of neural spine elongation, making it unique compared with other early-diverging iguanodontians (those branching earlier than Ankylopollexia). Of the taxa with tall neural spines, four in this study exceeded the upper 95% confidence interval for the ratio value in their ancestral node (Appendix S1; Fig. S31, Table S7). These were *Rhabdodon priscus* (by 26%), *Hypselospinus fittoni* (by 7%), *Ouranosaurus nigeriensis* (by 31%) and *Hypacrosaurus altispinus* (by 90%). The ancestral node of the sister taxa *Istiorachis macarthurae* and *Ouranosaurus nigeriensis* also shows a marked increase above the upper 95% confidence interval of the previous node. These are examples of particularly exaggerated hyperelongation, although it should be noted that the ancestral state for *Hypacrosaurus* might change if hadrosaurs were more completely sampled. *Morelladon beltrani* and *Istiorachis macarthurae* are within the 95% confidence intervals of the ancestral node and may therefore represent the upper end of normal variation in neural spine height rather than an autapomorphic episode of hyperelongation.

There are some caveats that may have affected the results of the reconstruction of ancestral states. One-third of the taxa used in the phylogenetic analysis required pruning given that there were no available data on their neural spine heights, and the number of taxa with data was particularly low in the middle Cretaceous.

The  $\log_{10}$  transformed bivariate plot (Fig. 19) of centrum height regressed against total body mass is highly correlated ( $R^2 = 0.833$ ), as would be expected. However, the  $\log_{10}$  transformed plot of Nh/Ch regressed against body mass showed low correlation between the two variables ( $R^2 = 0.245$ ) and demonstrates a wider variation in relative neural spine height in ankylopollexians and more deeply nested taxa than in the earlier diverging iguanodontians and neornithischians (Fig. 20). A  $\log_{10}$  transformed bivariate plot of the gracility index (Nh/Nw)

regressed against body mass also showed low correlation ( $R^2 = 0.4879$ ) (Appendix S1; Fig. S29). Some hadrosaurids such as *Edmontosaurus regalis* and *Parasaurolophus walkeri* had relatively tall centra (Fig. 19; E.r., P.w.); this would have exaggerated a relatively low value for the Nh/Ch ratio.

## DISCUSSION

### *Cervical vertebra of Istiorachis macarthurae*

The cervical vertebra possesses an anterior process at the base of the neural spine and an interpostzygapophyseal fossa posteriorly leading into a narrow tube-like structure (Fig. 3G). If the adjacent vertebrae were similarly constructed the process and fossa would have been closely apposed. These features most probably represent osteological correlates for a ligament and most closely match those marking the origin and insertion points of the unpaired and discontinuous ligamentum elasticum interlaminare. This ligament is found in all extant vertebrates with a tail (Reisdorf & Wuttke 2012), including crocodylians (Frey 1988) and avian dinosaurs (Boas 1929), and by inference (using extant phylogenetic bracketing) was also present in all non-avian dinosaurs. In Aves, the osteological correlates of the ligamentum elasticum interlaminare range from roughened tuberosities to facets, fossae or foveae (Baumer & Witmer 1993). The primary function of the ligamentum elasticum interlaminare in this group is to reduce muscle exertion to maintain neck posture, which is usually an S shape (Böhmer *et al.* 2020), and the ligament is well-developed in the extant ratite *Rhea americana* (Tsuihiji 2004). An S-shaped cervical spinal column is present in at least some, if not all, iguanodontians and was described in *Tenontosaurus tilletti* (Forster 1990) and RBINS R57 (Norman 1986), in which the centra of anterior cervical vertebrae are shorter ventrally than dorsally, but the reverse is seen in the posterior vertebrae. This ligament has also been proposed as an important part of the ligamentous system in sauropod necks (Tsuihiji 2004). Although conjectural, the findings in *Istiorachis macarthurae* of pronounced osteological correlates in a posterior and elongate cervical vertebra, could be explained by a relatively long, S-shaped neck.

### *Temporal & geographic distribution of neural spine elongation & hyperelongation in iguanodontians*

The results of this analysis demonstrate that relative neural spine elongation (measured as Nh/Ch) is not correlated with body mass in iguanodontian dinosaurs and instead finds that some iguanodontians had



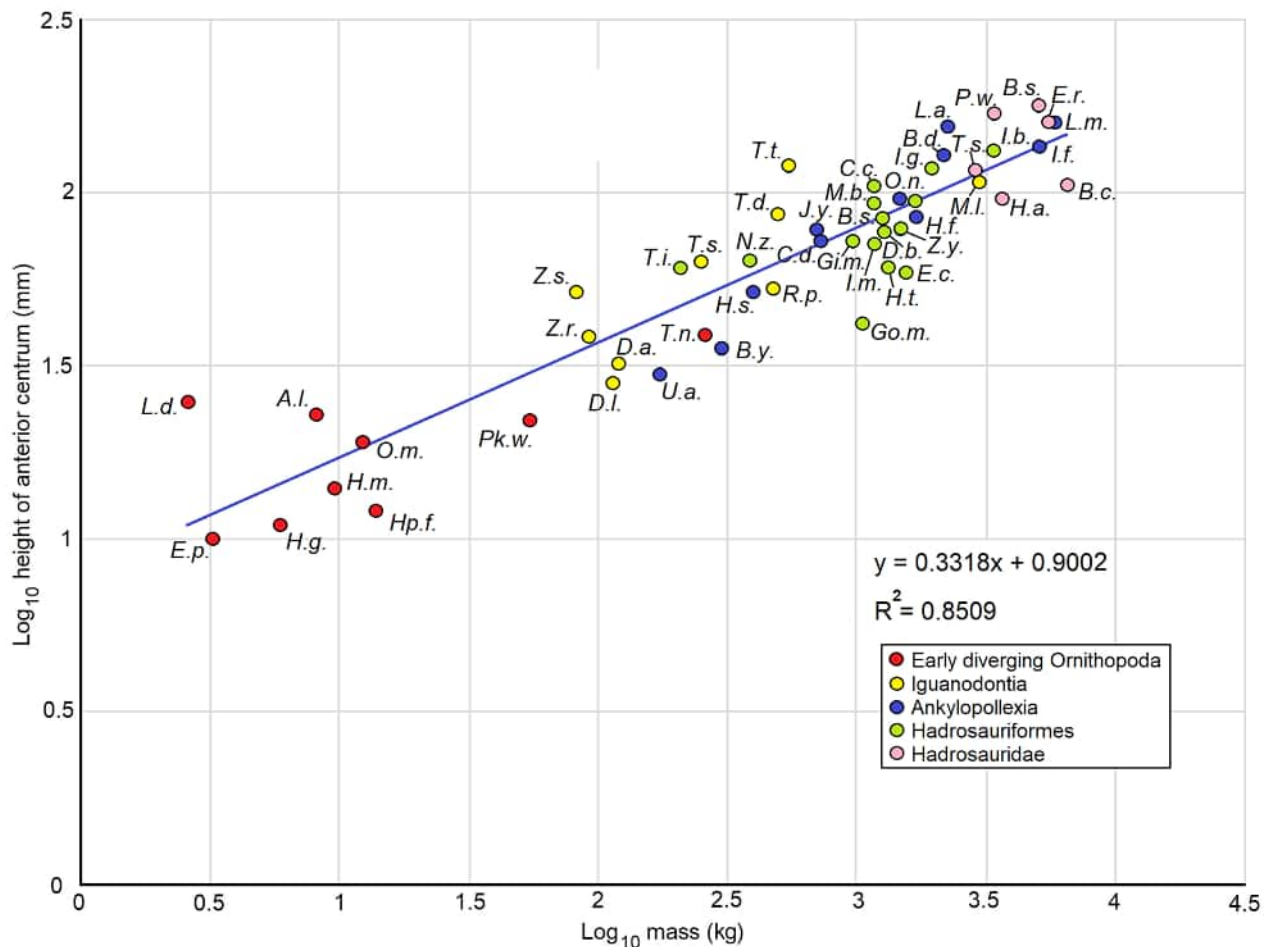


**FIG. 19.** Log<sub>10</sub> transformed bivariate plot of body mass (kg) vs the dorsoventral height of the anterior articular surface of a posteriorly situated dorsal centrum (mm) from iguanodontian and early diverging ornithischians. The blue line represents the linear regression described by the formula. Abbreviations: A.l., *Agilisaurus louderbacki*; Ba.s., *Barsboldia sicinskii*; B.c., *Brachylophosaurus canadensis*; B.d., *Barilium dawsoni*; B.j., *Bactrosaurus johnsoni*; B.s., *Brighstoneus simmondsi*; B.y., *Bolong yixianensis*; C.c., *Comptonatus chasei*; C.d., *Camptosaurus dispar*; D.a., *Dryosaurus altus*; D.b., RBINS R57; D.l., *Dysalotosaurus lettowvorbecki*; E.c., *Eolambia caroljonesa*; E.p., *Eocursor parvus*; E.r., *Edmontosaurus regalis*; Gi.m., *Gilmoresaurus mongoliensis*; Go.m., *Gobihadros mongoliensis*; H.a., *Hypacrosaurus altispinus*; Hd.f., *Hypsilophodon foxii*; H.f., *Hypselospinus fittoni*; H.g., *Haya griva*; H.m., *Hexinlusaurus multidens*; H.s., *Hippodraco scutodens*; H.t., *Huehuecanauhtlus tiquichensis*; I.b., *Iguanodon bernissartensis*; I.m., *Istiorachis macarthurae*; I.f., *Iguanacolossus fortis*; I.g., *Iguanodon galvensis*; J.y., *Jinzhousaurus yangi*; L.a., *Lurdusaurus arenatus*; L.d., *Lesothosaurus diagnosticus*; L.m., *Lanzhousaurus magnidens*; M.b., *Morelladon beltrani*; M.l., *Muttaborrasaurus langdoni*; N.z., *Nanyangosaurus zhugei*; O.m., *Orodromeus makelai*; O.n., *Ouranosaurus nigeriensis*; P.w., *Parasaurolophus walkeri*; Pk.w., *Parksosaurus warreni*; R.p., *Rabdodon priscus*; T.d., *Tenontosaurus dossi*; T.i., *Tethyshadros insularis*; T.n., *Thescelosaurus neglectus*; T.s., *Talenkauen santacrucensis*; T.si., *Taninus sinensis*; T.t., *Tenontosaurus tilletti*; U.a., *Uteodon aphanocetes*; Z.r., *Zalmoxes robustus*; Z.s., *Zalmoxes shqiperorum*; Z.y., *Zhanghenglong yangchengensis*.

hyperelongated neural spines, some had elongated neural spines, and others had relatively short neural spines. A general elongation of neural spines occurred after the Jurassic–Cretaceous boundary, but throughout the Early Cretaceous there was a range of taxa with each of these three character states. Taxa with elongate, hyperelongate and short neural spines appear to have been living alongside each other in Early Cretaceous ecosystems. For example, *Hypselospinus fittoni* and *Barilium dawsoni* are both from the Valanginian of the Wealden Group of southern

England, but the former has elongated neural spines relative to its ancestral node ( $Nh/Ch = 3.7$ ; above the 95% confidence interval for its ancestral condition), while the latter, a larger animal, had much shorter neural spines ( $Nh/Ch = 2.6$ , a value similar to that of its ancestral node). Mantell (1851) also found a series of six iguanodontian anterior caudal vertebrae in the late Valanginian Wealden Group, which show relatively long neural spines ( $Nh/Ch$  c. 4) with a similar ratio to *Hypselospinus fittoni*, and that appear to maintain their height through the

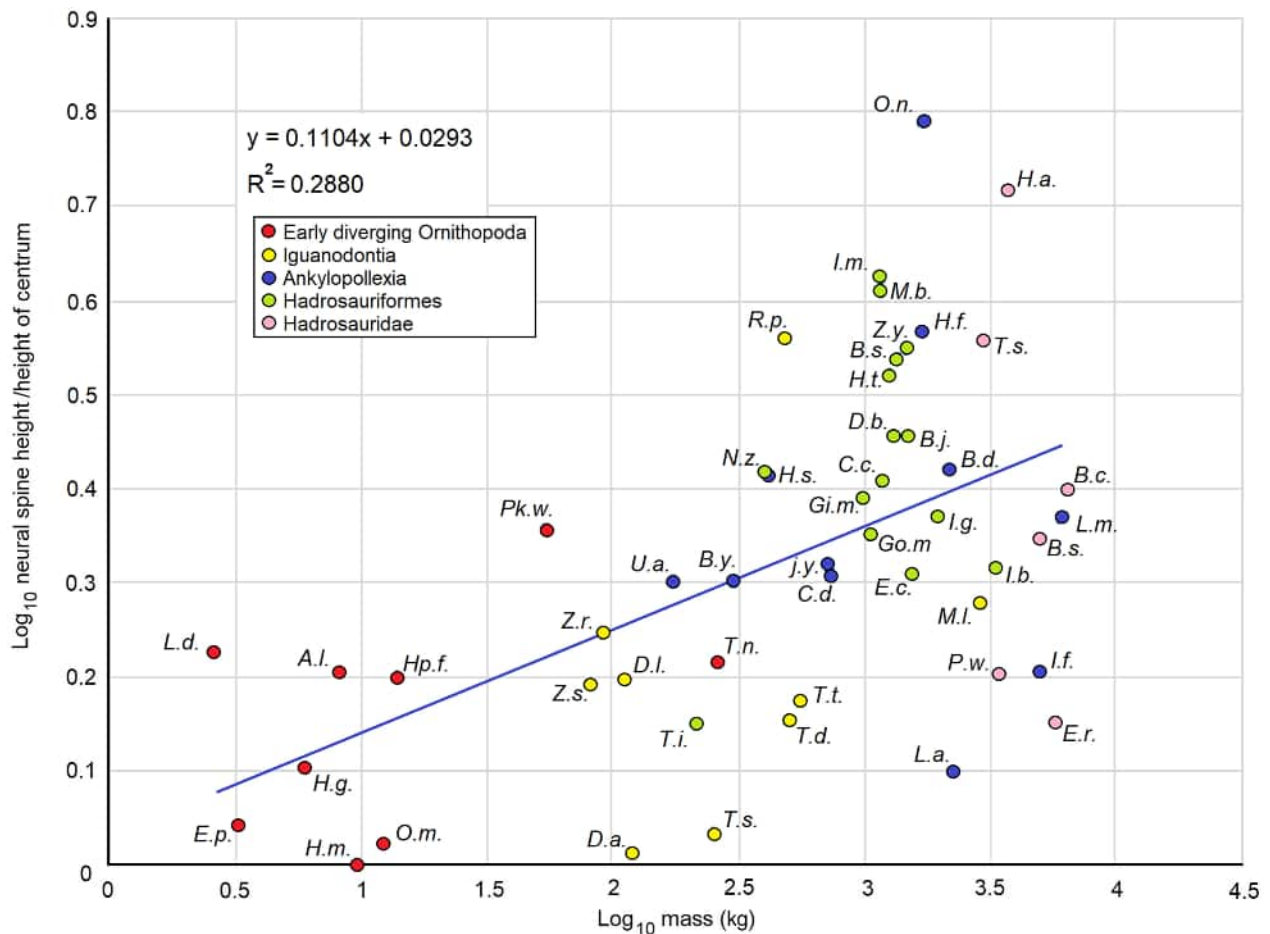


**FIG. 20.**  $\text{Log}_{10}$  transformed bivariate plot of body mass (kg) vs the neural spine to centrum height ratio (Nh/Ch), of iguanodontian and early diverging ornithischians. The blue line represents the linear regression described by the formula. *Abbreviations:* For names of taxa refer to Figure 19.

series, perhaps indicating another taxon with relatively elongate neural spines. A similar phenomenon is observed in the broadly contemporaneous (Joeckel *et al.* 2023) Yellow Cat Member of the Cedar Mountain Formation in Utah, USA. *Hippodraco* had neural spine lengths predicted by its ancestral values (Nh/Ch = 2.6), while *Iguanacolossus* appears to have had autapomorphically short neural spines (Nh/Ch = 1.6, a value lower than the 95% confidence interval for the ancestral value). Scheetz *et al.* (2010) reported bones of a specimen as large as *Iguanodon bernissartensis* from the base of the Cedar Mountain Formation in Utah with dorsal vertebrae with an Nh/Ch ratio of 5.5, perhaps indicating another taxon with hyperelongate neural spines. Slightly later in the Cretaceous, in the Barremian Wessex Formation of the Isle of Wight, *Istiorachis* had hyperelongate neural spines (Nh/Ch = 4.3), *Iguanodon* appears to have had short neural spines relative to its ancestral node (Nh/Ch = 2.6), while *Brighstoneus* (Nh/Ch = 3.3) and *Comptonatus*

(Nh/Ch = 2.6) have neural spine lengths predicted by their ancestral values. The Aptian of Niger also supported the iguanodontians *Ouranosaurus nigeriensis* with hyperelongate neural spines (Taquet 1976) alongside *Lurdusaurus arenatus* with much shorter neural spines (Taquet & Russell 1999). It is possible that this pattern continued into the Late Cretaceous, but taxon sampling is currently too poor, and too few hadrosaurs have been sampled in this phylogenetic analysis to draw robust conclusions.

#### *Implications for the function of elongate dorsal neural spines*

The generalized and relatively restrained increase in neural spine height at the base of Ankylopollexia contrasts with the development of more exaggerated structures in several iguanodontian taxa, and the reversion to shorter neural spine lengths in others, indicating that the

function of the neural spines in iguanodontian dinosaurs may have been pluralistic and complex. Ankylopollexians represent an important stage in iguanodontian evolution in which size and body mass was increasing, probably associated with the adoption of bulk herbivory (Benson *et al.* 2014). Maidment & Barrett (2014) identified five osteological correlates for ornithischian quadrupedality, at least four of which evolved in a stepwise manner close to the base of Ankylopollexia, suggesting that quadrupedality evolved near the base of this group (Poole 2022). This is also supported by ichnological discoveries of quadrupedal gait in smaller ornithopod trackways close to the Jurassic–Cretaceous boundary (Pérez-Lorente *et al.* 1997; Die-drich 2004; Hornung *et al.* 2012; Castanera *et al.* 2013). Osteological correlates for quadrupedality are well developed in hadrosauriforms and hadrosaurids, strongly suggesting that they were quadrupedal (Barrett & Maidment 2017) or facultatively bipedal, while earlier diverging taxa may have had variable gaits, probably being facultative quadrupeds (Dempsey *et al.* 2023). Quadrupedality requires a horizontally orientated spinal column and results in increased bending moments about the pelvic girdle. Although longitudinally arrayed ossified tendons on the dorsal neural spines are plesiomorphic for Ornithischia (Organ 2006), ankylopollexians developed epaxial ossified tendons arranged in a double (or more) lattice (Poole 2022). Although the function of ossified tendons has not been fully resolved, Ostrom (1964) considered that the primary function of the lattice was to counteract compressive or tensile stresses, which in iguanodontians (then considered mostly bipedal) were maximal close to the hind limbs, where the bending moments were greatest. Ostrom (1964) suggested that epaxial ossified tendons stiffened the vertebral column against buckling under the stresses of large body size. This was named the ‘postural hogging hypothesis’ by Organ (2006), whose work on the biomechanics of ossified tendons showed that a lattice stiffened the spine more efficiently than the plesiomorphic condition and was used to passively support the epaxial musculature in maintaining a more horizontally positioned vertebral column. The ossified tendons functioned to distribute forces in the same way as the cross-struts of a cantilever bridge, and the taller the neural spines, assuming the lattice architecture also became taller, the greater the proportion of the forces transmitted by the tendons that would be compressive (Organ 2006), therefore helping to counter the tensile forces due to postural hogging. Tall neural spines would also have increased the efficiency of the supraspinous ligament. Alternatively, due to the increased efficiency in bending moments produced by longer neural spines (Christian & Preuschoft 1996; Organ 2006), the dinosaur could reduce the epaxial muscle bulk and therefore its body mass, which may also have given it an evolutionary

advantage through reducing the need for resources or increasing running speed.

In many iguanodontians the neural spines tend to be tallest on the posterior dorsal vertebrae, as in *Bactrosaurus johnsoni* (Gilmore 1933), *Eolambia caroljonesa* (McDonald *et al.* 2012), and *Tenontosaurus tilletti* (Forster 1990), while in others, such as *Iguanodon bernissartensis* (Norman 1980) and RBINS R57 (Norman 1986), the difference is less marked although still evident. In some, the long neural spines continue over the haunches to include the sacral and proximal caudal vertebrae; for example, *Bactrosaurus johnsoni* (Godefroit *et al.* 1998), *Hypselospinus fittoni* (Norman 2015), *Brighstoneus simmondsi* (Lockwood *et al.* 2021) and *Istiorachis macarthurae*. These examples fit the model of the postural hogging hypothesis and could therefore suggest that elongate neural spines evolved to help support the body during locomotion as large body size and quadrupedality evolved.

From an evolutionary perspective, it is not clear why elongate dorsal neural spines did not appear more often, if they provided a mechanically efficient solution to the postural hogging hypothesis by augmenting bending moments and providing an increased and taller surface area for ossified epaxial tendons. Throughout the Cretaceous the variation in Nh/Ch ratio remained high. Mature hadrosaurids were almost certainly habitual quadrupeds and yet some, such as *Edmontosaurus regalis* and *Parasaurolophus walkeri*, had very low Nh/Ch ratios (1.4 and 1.6, respectively). In these two hadrosaurids, representing Saurolophinae and Lambeosaurinae, respectively, the neural spines are quite elongate as demonstrated by their gracility index (Appendix S1; Fig. S29), and *Parasaurolophus walkeri* is usually reconstructed as having some sort of sail structure along the back. The Nh/Ch ratio is, to some degree, misleading in these very large taxa, given that the centra are particularly robust and anteroposteriorly compressed (Fig. 19), as also seen in *Iguanodon bernissartensis* and *Barilium dawsoni*. This could be a scaling feature, but a taller centrum would also increase the bending moment (Christian & Preuschoft 1996), perhaps providing an alternative or secondary method of coping with the increased compressive and tensile stresses concomitant with being a quadrupedal megaherbivore. However, other hadrosaurids of comparable mass such as *Hypacrosaurus altispinus* and *Brachylophosaurus canadensis* do not appear to have adopted this approach.

Hyperelongation of neural spines in iguanodontians is recorded in the Early Cretaceous of Europe, North America and Africa, and the Late Cretaceous of Asia and North America, occurring in some 10% of the non-hadrosaurid iguanodontian taxa for which there are data. The spatial and time separation, together with the ancestral traits cladogram (Fig. 18) show that these were sometimes





**FIG. 21.** *Istiorachis chasei* gen. et sp. nov. (MIWG 6643). Life restoration. Original artwork by James Brown.

isolated, autapomorphic events. The most exaggerated hyperelongate dorsal neural spines of *Ouranosaurus nigeriensis* and *Hypacrosaurus altispinus* are tallest in the middle dorsal vertebrae, where they would have had the least biomechanical utility, suggesting that in some taxa, an alternative or pluralistic explanation for their function is needed. They also shared ecosystems with iguanodontian taxa that lacked hyperelongate neural spines, again making it less likely that they served a vital physiological function.

Non-mechanical hypotheses for tall neural spines can be considered in light of our results. Earlier theories of fat storage can be rejected because neural spines play no role in camelids (Endo *et al.* 2000), and the *Bison bison* hump has no role in fat storage. While the thermoregulatory function of sails remains debated, the appearance of elongated neural spines occurred at the Jurassic–Cretaceous boundary (Fig. 18), with subsequent examples of hyperelongation being rare and not specifically associated with Late Cretaceous cooling or the Cretaceous thermal maximum (Fig. 18; Huber *et al.* 2018), although data for the latter are limited. This leaves either sexual signalling or visual species signalling as the most compelling explanations for neural spine hyperelongation. Given that characters that are exaggerated beyond practical function in extant vertebrates are invariably sexually selected (Thomkins *et al.* 2010), it seems probable that sexual selection is the most likely hypothesis for hyperelongation. Among iguanodontians there is little convincing evidence for sexual dimorphism skeletally, except perhaps size in *Maiasaura peeblesorum* (Saitta *et al.* 2020), although sexual selection of an exaggerated character does not necessarily imply that it will be expressed

dimorphically (Kneel & Sampson 2011; Hone & Naish 2013). In the Bernissart collection of some 30 complete individuals of *Iguanodon bernissartensis* no dimorphism has been identified (Norman 1980; Verdú *et al.* 2017). However, most iguanodontian taxa are represented by single specimens, and neural spines are often incomplete, leaving us with insufficient material to assess whether neural spine height may have played a sexually dimorphic role in some species. Elongation and hyperelongation of iguanodontian dorsal neural spines coincided with increasing taxonomic diversity, and species with differing neural spine lengths often coexisted in the same ecosystem. In such cases neural spine elongation may have contributed to species recognition even if only as a secondary function. Additionally, tall neural spines could have made individuals appear larger, which may have helped to ward off predators or intraspecific rivals (Fig. 21).

## CONCLUSION

In recent years knowledge of the Isle of Wight Wealden Group dinosaur diversity has increased with the addition of the iguanodontians *Brighstoneus simmondsi* (Lockwood *et al.* 2021) and *Comptonatus chasei* (Lockwood *et al.* 2024), the ornithomimid *Vectidromeus insularis* (Longrich *et al.* 2024), the ankylosaurian *Vectipelta barretti* (Pond *et al.* 2023), the dromaeosaurid *Vectiraptor greeni* (Longrich *et al.* 2022) and the spinosaurids *Ceratosuchops inferodios* and *Riparovenator milnerae* (Barker *et al.* 2021), together with another possible spinosaurine (Barker *et al.* 2022). Other work on its macro- and microvertebrate

fossils has resulted in the Wessex Formation having one of the world's most taxonomically diverse non-marine Early Cretaceous vertebrate assemblages (Sweetman 2007, 2008, 2009; Sweetman & Gardner 2012; Penn & Sweetman 2023). This study describes a new iguanodontian taxon with hyperelongate neural spines and shows that a general increase in neural spine height was associated with the origin of Ankylopollexia at the Jurassic–Cretaceous boundary. Relative neural spine height in dorsal vertebrae is shown to be highly variable on a global and local basis. It appears probable that the function of elongate neural spines was pluralistic and may have included biomechanical advantage, sexual signalling and interspecies visual signalling. However, the wide variation in relative neural spine ratios means that a complete answer for neural spine function in iguanodontian dinosaurs remains elusive.

**Acknowledgements.** We are indebted to Dr Martin Munt and the staff at Dinosaur Isle Museum, Isle of Wight, especially Simon Penn and Alex Peaker for the enormous amount of time and effort afforded to this project. We acknowledge the late Nicholas Chase for finding, excavating and donating specimen MIWG 6643. We are also extremely grateful to Dr Colin Palmer for his helpful advice on biomechanics and Dr David Hone for a discussion on visual signalling. A big thank you to James Brown for his skilful artwork. Many thanks to Martyn Horne for his help and assistance with preparation, and local collectors Mick Green, Mark Penn, Fiona Wight, Shaun Smith, Andrew Cocks and Megan Jacobs for supporting the Isle of Wight iguanodontian project. Our thanks to two anonymous reviewers and editors Prof. Paul Barrett and Dr Sally Thomas for their very helpful comments, which greatly improved this paper. The programme TNT is made freely available courtesy of the Willi Hennig Society. This paper is a contribution to the Natural History Museum's Evolution of Life Research Theme.

**Author contributions.** **Conceptualization** JAF Lockwood (JAFL), SCR Maidment (SCRM) and DM Martill (DMM); **Data Curation** JAFL; **Formal Analysis** JAFL, SCRM; **Investigation** JAFL, SCRM; **Software** JAFL, SCRM; **Supervision** SCRM, DMM; **Visualization**, JAFL, SCRM; **Writing – Original Draft Preparation** JAFL; **Writing – Review & Editing** JAFL, SCRM, DMM.

## DATA ARCHIVING STATEMENT

Data from this study covering neural spine full data (.xlsx) and ancestral states reconstruction; Nh/Ch ratios (.cvs), age data (.txt), R code (.R), tree (.nex) are available in the Dryad Digital Repository: <https://doi.org/10.5061/dryad.v6wvwpzh78>. This published work and the nomenclatural act it contains, have been registered in ZooBank: <https://zoobank.org/References/18c86de7-5a00-46e9-989b-5b499a5ed456>.

Editor. Paul Barrett

## SUPPORTING INFORMATION

Additional Supporting Information can be found online (<https://doi.org/10.1002/spp2.70034>):

**Appendix S1.** Figures and metrics of all axial and pelvic elements of *Istiorachis macarthurae*, and nodal values and positions for the ancestral states reconstruction. Includes Figures S1–S31 and Tables S1–S7.

**Appendix S2.** *Istiorachis macarthurae* matrix in tnt format.

## REFERENCES

- Allen, P. and Wimbledon, W. A. 1991. Correlation of NW European Purbeck-Wealden (non-marine Lower Cretaceous) as seen from the English type-areas. *Cretaceous Research*, **12**, 511–526.
- Bailey, J. B. 1997. Neural spine elongation in dinosaurs: sail backs or buffalo-backs. *Journal of Paleontology*, **71**, 1124–1146.
- Bapst, D. W. 2012. Paleotree: an R package for paleontological and phylogenetic analyses of evolution. *Methods in Ecology & Evolution*, **3**, 803–807.
- Barker, C. T., Hone, D. W. E., Naish, D., Cau, A., Lockwood, J. A. F., Foster, B., Clarkin, C. E., Schneider, P. and Gostling, N. J. 2021. New spinosaurids from the Wessex Formation (Early Cretaceous, UK) and the European origins of Spinosauridae. *Scientific Reports*, **11**, 19340.
- Barker, C. T., Lockwood, J. A., Naish, D., Brown, S., Hart, A., Tulloch, E. and Gostling, N. J. 2022. A European giant: a large spinosaurid (Dinosauria: Theropoda) from the Vectis Formation (Wealden Group, Early Cretaceous), UK. *PeerJ*, **10**, e13543.
- Baron, M. G., Norman, D. B. and Barrett, P. M. 2017. Postcranial anatomy of *Lesothosaurus diagnosticus* (Dinosauria: Ornithischia) from the Lower Jurassic of southern Africa: implications for basal ornithischian taxonomy and systematics. *Zoological Journal of the Linnean Society*, **179**, 125–168.
- Barrett, P. M. 2016. A new specimen of *Valdosaurus canaliculatus* (Ornithopoda: Dryosauridae) from the Lower Cretaceous of the Isle of Wight, England. *Memoirs of Museum Victoria*, **74**, 29–48.
- Barrett, P. M. and Maidment, S. C. R. 2017. The evolution of ornithischian quadrupedality. *Journal of Iberian Geology*, **43**, 363–377.
- Barrett, P. M., McGowan, A. J. and Page, V. 2009a. Dinosaur diversity and the rock record. *Proceedings of the Royal Society B*, **276**, 2667–2674.
- Barrett, P. M., Butler, R. J., Wang, X.-L. and Xu, X. 2009b. Cranial anatomy of the iguanodontoid ornithopod *Jinzhousaurus yangi* from the Lower Cretaceous Yixian Formation of China. *Acta Palaeontologica Polonica*, **54**, 35–48.
- Batten, D. J. 2011. Wealden geology. 7–14. In Batten, D. J. (ed.) *English Wealden fossils*. The Palaeontological Association. Field Guide to Fossils 14. 780 pp.
- Batten, D. J. and Austen, P. A. 2011. The Wealden of Southeast England. 15–51. In Batten, D. J. (ed.) *English Wealden fossils*. The Palaeontological Association. Field Guide to Fossils 14. 780 pp.

- Baumel, J. J. and Witmer, L. M. 1993. Osteologia. 45–132. In Baumel, J. J., King, A. S., Breazile, J. E., Evans, H. E. and Van den Berge, J. C. (eds) *Handbook of avian anatomy: Nomina Anatomica Avium*. Nuttall Ornithological Club. 779 pp.
- Baur, G. 1891. Remarks on the reptiles generally called Dinosauria. *American Naturalist*, **25**, 434–454.
- Bennett, S. C. 1996. Aerodynamics and thermoregulatory function of the dorsal sail of *Edaphosaurus*. *Paleobiology*, **22**, 496–506.
- Benson, R. B. J., Campione, N. E., Carrano, M. T., Mannion, P. D., Sullivan, C., Upchurch, P. and Evans, D. C. 2014. Rates of dinosaur body mass evolution indicate 170 million years of sustained ecological innovation on the avian stem lineage. *PLoS Biology*, **12** (5), e1001853.
- Bertozzo, F., Della Vecchia, F. M. and Fabbri, M. 2017. The Venice specimen of *Ouranosaurus nigeriensis* (Dinosauria, Ornithopoda). *PeerJ*, **5**, e3403.
- Boas, J. E. V. 1929. Biologisch-anatomische studien über den hals der vögel. *Kongelige Danske Videnskabernes Selskabs Skriftet*, **9**, 101–222.
- Böhmer, C., PrevotEAU, J., Durie, O. and Abourachid, A. 2020. Gulper, ripper and scrapper: anatomy of the neck in three species of vultures. *Journal of Anatomy*, **236**, 701–723.
- Bonsor, J. A., Lockwood, J. A. F., Vasco Leite, J., Scott-Murray, A. and Maidment, S. C. R. 2023. The osteology of the holotype of the British iguanodontian dinosaur *Mantellisaurus atherfieldensis*. *Monographs of the Palaeontographical Society*, **177** (665), 1–63.
- Borinder, N. H., Poropat, S. F., Campione, N. E., Wigren, T. and Kear, B. P. 2021. Postcranial osteology of the basally branching hadrosauroid dinosaur *Tanais sinensis* from the Upper Cretaceous Wangshi Group of Shandong, China. *Journal of Vertebrate Paleontology*, **41** (1), e1914642.
- Bramwell, C. D. and Felgett, P. B. 1973. Thermal regulation in sail lizards. *Nature*, **242**, 203–205.
- Brett-Surman, M. K. and Wagner, J. R. 2007. Discussion of character analysis of the appendicular anatomy in Campanian and Maastrichtian North American hadrosaurids: variation and ontogeny. 135–169. In Carpenter, K. (ed.) *Horns and beaks: Ceratopsian and ornithomimid dinosaurs*. Indiana University Press. 384 pp.
- Brown, B. 1913a. A new trachodont dinosaur, *Hypacrosaurus*, from the Edmonton Cretaceous of Alberta. *Bulletin of the American Museum of Natural History*, **32**, 395–406.
- Brown, B. 1913b. The skeleton of *Saurolophus*, a crested duck-billed dinosaur from the Edmonton Cretaceous. *Bulletin of the American Museum of Natural History*, **32**, 387–393.
- Butler, R. J., Brusatte, S. J., Reich, M., Nesbitt, S. J., Schoch, R. R. and Hornung, J. J. 2011. The sail-backed reptile *Ctenosaurus* from the latest Early Triassic of Germany and the timing and biogeography of the early archosaur radiation. *PLoS One*, **6** (10), e25693.
- Caro, T. and Allen, W. L. 2017. Interspecific visual signalling in animals and plants: a functional classification. *Philosophical Transactions of the Royal Society B*, **372**, 20160344.
- Carpenter, K. and Wilson, Y. 2008. A new species of *Camptosaurus* (Ornithopoda: Dinosauria) from the Morrison Formation (Upper Jurassic) of Dinosaur National Monument, Utah, and a biomechanical analysis of its forelimb. *Annals of Carnegie Museum*, **76**, 227–263.
- Case, E. C. 1910. New or little known reptiles and amphibians from the Permian (?) of Texas. *Bulletin of the American Museum of Natural History*, **28**, 163–181.
- Castanera, D., Vila, B., Razzolini, N. L., Falkingham, P. L., Canudo, J. I., Manning, P. L. and Galobart, A. 2013. Manus track preservation bias as a key factor for assessing trackmaker identity and quadrupedalism in basal ornithopods. *PLoS One*, **8** (1), e54177.
- Christian, A. and Preuschoft, H. 1996. Deducing the body posture of extinct large vertebrates from the shape of the vertebral column. *Palaeontology*, **39**, 801–812.
- Cope, E. D. 1875. On the Batrachia and Reptilia of Costa Rica. *Journal of the Academy of Natural Sciences of Philadelphia*, **8**, 93–154.
- Cope, E. D. 1877. Descriptions of extinct vertebrata from the Permian and Triassic formations of the United States. *Proceedings of the American Philosophical Society*, **17**, 182–193.
- Cope, E. D. 1882. Third contribution to the history of the Vertebrata of the Permian formation of Texas. *Proceedings of the American Philosophical Society*, **20**, 447–461.
- Dempsey, M., Maidment, S. C. R., Hedrick, B. P. and Bates, K. T. 2023. Convergent evolution of quadrupedality in ornithischian dinosaurs was achieved through disparate forelimb muscle mechanics. *Proceedings of the Royal Society B*, **290**, 20222435.
- Denzer, W., Campbell, P. D., Glässer-Trobisch, A. and Kocks, A. 2020. Dragons in neglect: taxonomic revision of the Sulawesi sailfin lizards of the genus *Hydrosaurus* Kaup, 1828 (Squamata, Agamidae). *Zootaxa*, **4747**, 275–301.
- Diedrich, C. 2004. New important iguanodontid and theropod trackways of the tracksite Obernkirchen in the Berriasian of NW Germany and megatracksite concept of Central Europe. *Ichnos*, **11**, 215–228.
- Endo, H., Cao, G., Borjihan, D., Borjihan, E., Dugarjav, M. and Hayashi, Y. 2000. Hump attachment structure of the two-humped camel (*Camelus bactrianus*). *Journal of Veterinary Medical Science*, **62**, 521–524.
- Flóres, G. A., Wrobel, R. L. C., Kalogirou, S. A. and Tassoub, S. A. 1999. A thermal model for reptiles and pelycosaurs. *Journal of Thermal Biology*, **24**, 1–13.
- Forster, C. A. 1990. The postcranial skeleton of the ornithomimid dinosaur *Tenontosaurus tilletti*. *Journal of Vertebrate Paleontology*, **10**, 273–294.
- Frey, E. 1988. Anatomie des körperstammes von *Alligator mississippiensis* Daudin. *Stuttgarter Beiträge zur Naturkunde Serie A (Biologie)*, **424**, 1–106.
- Fuentes Vidarte, C., Mejjide Calvo, M., Mejjide Fuentes, F. and Mejjide Fuentes, M. 2016. Un nuevo dinosaurio estiracosterno (Ornithopoda: Ankylopollexia) del Cretácico Inferior de España. *Spanish Journal of Palaeontology*, **31**, 407–446.
- Gale, A. S. 2019. *The Isle of Wight*. The Geologists' Association Guide 60. 174 pp.
- Gallina, P. A., Apesteguía, S., Canale, J. I. and Haluza, A. 2019. A new long-spined dinosaur from Patagonia sheds light on sauropod defence system. *Scientific Reports*, **9** (1), 1392.



- Galton, P. M. 1974. The ornithischian dinosaur *Hypsilophodon* from the Wealden of the Isle of Wight Bulletin of the British Museum (Natural History). *Geology*, **25**, 1–152.
- Galton, P. M. 1980. European Jurassic ornithopod dinosaurs of the families Hypsilophodontidae and Camptosauridae. *Neues Jahrbuch für Geologie und Paläontologie, Abhandlungen*, **160**, 73–95.
- Galton, P. M. 2012. *Hypsilophodon foxii* and other smaller bipedal ornithischian dinosaurs from the Lower Cretaceous of Southern England. 175–212. In Godefroit, P. (ed.) *Bernissart dinosaurs and Early Cretaceous terrestrial ecosystems*. Indiana University Press, 648 pp.
- Gasca, J. M., Canudo, J. I. and Morenzo-Azanza, M. 2014. On the diversity of Iberian iguanodont dinosaurs: new fossils from the lower Barremian, Teruel province, Spain. *Cretaceous Research*, **50**, 264–272.
- Gasulla, J. M., Escaso, F., Narváez, I., Otega, F. and Sanz, J. L. 2015. A new sail-backed styracosternan (Dinosauria: Ornithopoda) from the Early Cretaceous of Morella, Spain. *PLoS One*, **10**, e0144167.
- Gasulla, J. M., Escaso, F., Narváez, I., Sanz, J. L. and Ortega, F. 2022. New *Iguanodon bernissartensis* axial bones (Dinosauria, Ornithopoda) from the Early Cretaceous of Morella, Spain. *Diversity*, **14** (63), 1–16.
- Gates, T. A., Tsogtbaatar, K., Zanno, L. E., Chinzorig, T. and Watabe, M. 2018. A new iguanodontian (Dinosauria: Ornithopoda) from the Early Cretaceous of Mongolia. *PeerJ*, **6**, e5300.
- Gilmore, C. W. 1909. Osteology of the Jurassic reptile *Camptosaurus*, with a revision of the species of the genus, and descriptions of two new species. *Proceedings of the United States National Museum*, **36**, 197–332.
- Gilmore, C. W. 1933. On the dinosaurian fauna of the Iren Dabasu Formation. *Bulletin of the American Museum of Natural History*, **67**, 23–78.
- Godefroit, P., Dong, Z.-M., Bultynck, P., Li, H. and Feng, L. 1998. Sino-Belgian Cooperative Program. Cretaceous dinosaurs and mammals from Inner Mongolia: 1. New *Bactrosaurus* (Dinosauria: Hadrosauridae) material from Iren Dabasu (Inner Mongolia, P.R. China). *Bulletin de l'Institut Royal des Sciences Naturelles du Belgique, Sciences de la Terre*, **68**, 3–70.
- Godefroit, P., Codrea, V. and Weishampel, D. B. 2009. Osteology of *Zalmoxes shqiperorum* (Dinosauria, Ornithopoda), based on new specimens from the Upper Cretaceous of Nalat-Vad (Romania). *Geodiversitas*, **31**, 525–553.
- Godefroit, P., Bolotsky, Y. L. and Lauters, P. 2012. A new saurolophine dinosaur from the latest Cretaceous of far eastern Russia. *PLoS One*, **7**, e36849.
- Goloboff, P. A. 2014. Extended implied weighting. *Cladistics*, **30**, 260–272.
- Goloboff, P. A. and Morales, M. 2023. TNT version 1.6, with graphical interface for MacOs and Linux, including new routines in parallel. *Cladistics*, **39**, 144–153.
- Guenter, M. F. 2007. Morphology and ontogeny of the postcranial skeleton of Hadrosauridae. PhD thesis. Earth and Environmental Science, The University of Pennsylvania, Philadelphia, Pennsylvania, USA. 210 pp.
- Hone, D. W. E. and Naish, D. 2013. The 'species recognition hypothesis' does not explain the presence and evolution of exaggerated structures in non-avian dinosaurs. *Journal of Zoology*, **290**, 172–180.
- Hooley, R. W. 1925. On the skeleton of *Iguanodon atherfieldensis* sp. nov., from the Wealden Shales of Atherfield (Isle of Wight). *Quarterly Journal of the Geological Society of London*, **81**, 1–61.
- Horner, J. R., Weishampel, D. B. and Forster, C. A. 2004. Hadrosauridae. 436–463. In Weishampel, D. B., Dodson, P. and Osmólska, H. (eds) *The Dinosauria*. University of California Press, Second edition. 861 pp.
- Hornung, J. J., Böhme, A., Van der Lubbe, T., Reich, M. and Richter, A. 2012. Vertebrate tracksites in the Obernkirchen Sandstone (late Berriasian, Early Cretaceous) of northwest Germany: their stratigraphical, palaeogeographical, palaeoecological, and historical context. *Paläontologische Zeitschrift*, **86**, 231–267.
- Huber, B. T., MacLeod, K. G., Watkins, D. K. and Coffin, M. F. 2018. The rise and fall of the Cretaceous hot greenhouse climate. *Global and Planetary Change*, **167**, 1–23.
- Huene, F. von 1923. Carnivorous Saurischia in Europe since the Triassic. *Bulletin of the Geological Society of America*, **34**, 449–458.
- Hutt, S., Naish, D., Martill, D. M., Barker, M. J. and Newberry, P. 2001. A preliminary account of a new tyrannosauroid theropod from the Wessex Formation (Cretaceous) of southern England. *Cretaceous Research*, **22**, 227–242.
- Huttenlocker, A. K., Mazierski, D. and Reisz, R. R. 2011. Comparative osteohistology of hyperelongate neural spines in the Edaphosauridae (Amniota: Synapsida). *Palaeontology*, **54**, 573–590.
- Ibrahim, N., Sereno, P. C., Sasso, C. D., Maganuco, S., Fabbri, M., Martill, D. M., Zouhri, S., Myhrvold, N. and Iurino, D. A. 2014. Semiaquatic adaptations in a giant predatory dinosaur. *Science*, **345**, 1613–1616.
- Ibrahim, N., Maganuco, S., Sasso, C. D., Fabbri, M., Audatore, M., Bindellini, G., Martill, D. M., Zouhri, S., Mattarelli, D. A., Unwin, D. M., Wiemann, J., Bonadonna, D., Amare, A., Jakubczak, J., Joger, U., Lauder, G. V. and Pierce, S. E. 2020. Tail-propelled aquatic locomotion in a theropod dinosaur. *Nature*, **581**, 67–70.
- Janensch, W. 1914. Übersicht über die Wirbeltierfauna der Tendaguru-Schichten (Overview of the vertebrate fauna of the Tendaguru beds). *Archiv für Biontologie*, **3**, 81–110.
- Janensch, W. 1955. Der Ornithopode *Dysalotosaurus* der Tendaguruschichten. *Palaeontographica-Supplementbände*, **7**, 105–176.
- Joeckel, R. M., Suarez, C. A., McLean, N. M., Möller, A., Ludwig, G. A., Suarez, M. B., Kirkland, J. I., Andrew, J., Kiesling, S. and Hatzell, G. A. 2023. Berriasian–Valanginian geochronology and carbon-isotope stratigraphy of the Yellow Cat Member, Cedar Mountain Formation, Eastern Utah, USA. *Geosciences*, **13** (2), 32.
- Kaup, J. J. 1828. Ueber *Hyaena*, *Uromastix*, *Basileiscus*, *Corythaeolus*, *Acontias*. *Isis von Oken*, **21**, 1144–1150.
- Klaver, C. and Böhme, W. 1992. The species of the *Chamaeleo cristatus* group from Cameroon and adjacent countries, West Africa. *Bonner Zoologische Beiträge*, **43**, 433–478.
- Knell, R. J. and Sampson, S. 2011. Bizarre structures in dinosaurs: species recognition or sexual selection? A response to Padian and Horner. *Journal of Zoology*, **283**, 18–22.

- Lambe, L. M. 1917. A new genus and species of crestless hadrosaur from the Edmonton Formation of Alberta. *The Ottawa Naturalist*, **31** (7), 65–73.
- Lambe, L. M. 1920. The hadrosaur *Edmontosaurus* from the Upper Cretaceous of Alberta. *Memoirs of the Geological Survey of Canada*, **102**, 1–79.
- Lattanzio, M. S. 2019. Delayed escape responses of male *Basiliscus plumifrons* (Squamata: Corytophanidae) during peak activity. *Phyllomedusa*, **18**, 185–193.
- Linnaeus, C. 1758. *Systema Naturae, sive regina tria naturae systematice proposita por classes, ordines, genera, species cum characteribus differentiis synonymis, locis*, Tenth edition. L. Salvii, Holmiae. 1384 pp.
- Lockwood, J. A. F., Martill, D. M. and Maidment, S. C. R. 2021. A new hadrosauriform dinosaur from the Wessex Formation, Wealden Group (Early Cretaceous), of the Isle of Wight, southern England. *Journal of Systematic Palaeontology*, **19**, 847–888.
- Lockwood, J. A. F., Martill, D. M. and Maidment, S. C. R. 2024. *Comptonatus chasei*, a new iguanodontian dinosaur from the Lower Cretaceous Wessex Formation of the Isle of Wight, southern England. *Journal of Systematic Palaeontology*, **22** (1), 2346573.
- Lockwood, J. A. F., Martill, D. M. and Maidment, S. C. R. 2025. Data from: the origins of neural spine elongation in iguanodontian dinosaurs and the osteology of a new sail-back styracosternan (Dinosauria: Ornithischia) from the Lower Cretaceous Wealden Group of England [dataset]. Dryad. <https://doi.org/10.5061/dryad.v6wwpzh78>
- Longrich, N. R., Martill, D. M. and Jacobs, M. L. 2022. A new dromaeosaurid dinosaur from the Wessex Formation (Lower Cretaceous, Barremian) of the Isle of Wight, and implications for European palaeobiogeography. *Cretaceous Research*, **134**, 105–123.
- Longrich, N. R., Martill, D. M., Munt, M., Green, M., Penn, M. and Smith, S. 2024. *Vectidromeus insularis*, a new hypsilophodontid dinosaur from the Lower Cretaceous Wessex Formation of the Isle of Wight, England. *Cretaceous Research*, **154**, 105707.
- Lydekker, R. 1889a. On the remains and affinities of five genera of Mesozoic reptiles. *Quarterly Journal of the Geological Society of London*, **45**, 41–59.
- Lydekker, R. 1889b. Notes on new and other dinosaur remains. *Geological Magazine*, **6** (8), 352–356.
- Maddison, W. P. and Maddison, D. R. 2015. Mesquite: a modular system for evolutionary analysis. Version 3.61. <https://www.mesquiteproject.org/>
- Maidment, S. C. M. and Barrett, P. M. 2014. Osteological correlates for quadrupedality in ornithischian dinosaurs. *Acta Palaeontologica Polonica*, **59**, 53–70.
- Maidment, S. C. R., Chappelle, K. E. J., Bonsor, J. A., Button, D. and Barrett, P. M. 2023. Osteology and relationships of *Cumnoria prestwichii* (Ornithischia: Ornithopoda) from the late Jurassic of Oxfordshire, UK. *Monograph of the Palaeontological Society*, **176** (644), 1–55.
- Mann, A. and Reisz, R. R. 2020. Antiquity of sail-backed neural spine hyper-elongation in mammal forerunners. *Frontiers of Earth Science*, **8**, 83.
- Mantell, G. A. 1851. *Petrifactions and their teachings; or a handbook to the gallery of organic remains of The British Museum*. Henry G. Bohn, London. 496 pp.
- Marsh, O. C. 1881. Principal characters of American Jurassic dinosaurs. Part IV. Spinal cord, pelvis, and limbs of *Stegosaurus*. *American Journal of Science Series*, **3** (21), 167–170.
- Martill, D. M. and Naish, D. 2001. *Dinosaurs of the Isle of Wight*. The Palaeontological Association Field Guide to Fossils 10. 433 pp.
- Maryńska, T. and Osmólska, H. 1981. First lambeosaurine dinosaur from the Nemegt Formation, Upper Cretaceous, Mongolia. *Acta Palaeontologica Polonica*, **26**, 243–255.
- McDonald, A. T. 2012a. The status of *Dollododon* and other basal iguanodonts (Dinosauria: Ornithischia) from the upper Wealden beds (Lower Cretaceous) of Europe. *Cretaceous Research*, **33**, 1–6.
- McDonald, A. T. 2012b. Phylogeny of basal iguanodonts (Dinosauria: Ornithischia): an update. *PLoS One*, **7**, e36745.
- McDonald, A. T., Bird, J., Kirkland, J. I. and Dodson, P. 2012. Osteology of the basal hadrosauroid *Eolambia caroljonesa* (Dinosauria: Ornithopoda) from the Cedar Mountain Formation of Utah. *PLoS One*, **7**, e45712.
- Meagher, M. 1986. *Bison bison*. *Mammalian Species*, **266**, 1–8.
- Naish, D. and Cau, A. 2022. The osteology and affinities of *Eotyrannus lengi*, a tyrannosauroid theropod from the Wealden Supergroup of southern England. *PeerJ*, **10**, e12727.
- Nesbitt, S. J. 2003. *Arizonasaurus* and its implications for archosaur divergence. *Proceedings of the Royal Society B*, **270**, 234–237.
- Norman, D. B. 1980. On the ornithischian dinosaur *Iguanodon bernissartensis* of Bernissart (Belgium). *Mémoires de l'Institut Royal des Sciences Naturelles de Belgique*, **178**, 1–105.
- Norman, D. B. 1986. On the anatomy of *Iguanodon atherfieldensis* (Ornithischia: Ornithopoda). *Bulletin de l'Institut Royal des Sciences Naturelles de Belgique Sciences de la Terre*, **56**, 281–372.
- Norman, D. B. 1998. On Asian ornithopods (Dinosauria, Ornithischia). 3. A new species of iguanodontid dinosaur. *Zoological Journal of the Linnean Society*, **122**, 291–348.
- Norman, D. B. 2002. On Asian ornithopods (Dinosauria: Ornithischia). 4. *Probactrosaurus Rozhdestvensky*, 1966. *Zoological Journal of the Linnean Society*, **136**, 113–144.
- Norman, D. B. 2010. A taxonomy of iguanodontians (Dinosauria: Ornithopoda) from the lower Wealden Group (Cretaceous: Valanginian) of southern England. *Zootaxa*, **2489**, 47–66.
- Norman, D. B. 2011. On the osteology of the lower Wealden (Valanginian) ornithopod *Barilium dawsoni* (Iguanodontia: Styracosterna). *Special Papers in Palaeontology*, **86**, 165–194.
- Norman, D. B. 2012. Iguanodontian taxa (Dinosauria: Ornithischia) from the Lower Cretaceous of England and Belgium. 175–212. In Godefroit, P. (ed.) *Bernissart dinosaurs and Early Cretaceous terrestrial ecosystems*. Indiana University Press. 648 pp.
- Norman, D. B. 2015. On the history, osteology, and systematic position of the Wealden (Hastings Group) dinosaur *Hypselospinus fittoni* (Iguanodontia: Styracosterna). *Zoological Journal of the Linnean Society*, **173**, 92–189.

- O'Gorman, E. J. and Hone, D. W. E. 2012. Body size distribution of the dinosaurs. *PLoS One*, **7** (12), e51925.
- Oldham, T. C. B. 1976. The plant debris beds of the English Wealden. *Palaeontology*, **19**, 437–502.
- Organ, C. L. 2006. Biomechanics of ossified tendons in ornithomimid dinosaurs. *Paleobiology*, **32**, 652–665.
- Ortega, F., Escaso, F. and Sanz, J. L. 2010. A bizarre, humped Carcharodontosauria (Theropoda) from the Lower Cretaceous of Spain. *Nature*, **467**, 203–206.
- Ostrom, J. H. 1964. A reconsideration of the paleoecology of hadrosaurian dinosaurs. *American Journal of Science*, **262**, 975–997.
- Ostrom, J. H. 1970. Stratigraphy and paleontology of the Cloverly Formation (Lower Cretaceous) of the Bighorn Basin area, Wyoming and Montana. *Peabody Museum Bulletin*, **35**, 1–234.
- Owen, R. 1842. Report on British fossil reptiles. Part II. 60–204. In British Association (ed.) *Report of the eleventh meeting of the British Association for the Advancement of Science, held at Plymouth in July 1841*. John Murray, London. <https://www.biodiversitylibrary.org/page/33377524>
- Padian, K. and Horner, J. R. 2011. The evolution of 'bizarre structures' in dinosaurs: biomechanics, sexual selection, social selection or species recognition? *Journal of Zoology*, **283**, 3–17.
- Parks, W. A. 1922. *Parasaurolophus walkeri*, a new genus and species of trachodont dinosaur. *University of Toronto Studies: Geological Series*, **13**, 5–32.
- Paul, G. S. 2016. *The Princeton field guide to dinosaurs*, Second edition. Princeton University Press, New Jersey, 360 pp.
- Penn, S. J. and Sweetman, S. C. 2023. Microvertebrate-rich gutter casts from the basal Wessex Formation (Wealden Group, Lower Cretaceous) of Dungeness Head, Dorset: insights into the palaeoecology and palaeoenvironment of a non-marine wetland. *Cretaceous Research*, **143**, 105397.
- Pereda-Suberbiola, X., Rui-Omeñaca, J. I., Fernández-Baldor, F. T., Maisch, M. W., Huerta, P., Contreras, R., Izquierdo, L. A., Huert, D. M., Montero, V. U. and Welle, J. 2011. A tall-spined ornithomimid dinosaur from the Early Cretaceous of Salas de los Infantes (Burgos, Spain). *Comptes Rendus Palevol*, **10**, 551–558.
- Pérez-Lorente, F., Cuenca-Bescós, G., Aurell, M., Canudo, J. I., Soria, A. R. and Ruiz-Omeñaca, J. I. 1997. Las Cerradillas tracksite (Berriasian, Galve, Spain): growing evidence for quadrupedal ornithomimids. *Ichnos*, **5**, 109–120.
- Persons, W. S. IV and Currie, P. J. 2011. Dinosaur speed demon: the caudal musculature of *Carnotaurus sastrei* and implications for the evolution of South American Abelisaurids. *PLoS One*, **6** (10), e25763.
- Pond, S., Strachan, S., Raven, T. J., Simpson, M. I., Morgan, K. and Maidment, S. C. R. 2023. *Vectipelta barretti*, a new ankylosaurian dinosaur from the Lower Cretaceous Wessex Formation of the Isle of Wight, UK. *Journal of Systematic Palaeontology*, **21**, 2210577.
- Poole, K. E. 2015. Phylogeny and biogeography of iguanodontian dinosaurs, with implications from ontogeny and an examination of the function of the fused carpal-digit I complex. PhD thesis. The Columbian College of Arts and Sciences of the George Washington University, St Louis, USA. 220 pp.
- Poole, K. E. 2022. Phylogeny of iguanodontian dinosaurs and the evolution of quadrupedality. *Palaeontologica Electronica*, **25** (3), a30.
- Prieto-Márquez, A. 2001. Osteology and variation of *Brachylophosaurus canadensis* (Dinosauria, Hadrosauridae) from the Upper Cretaceous Judith River Formation of Montana. Master's thesis, Montana State University, Bozeman, USA. 390 pp.
- Prieto-Márquez, A. and Norell, M. A. 2010. Anatomy and relationships of *Gilmoresaurus mongoliensis* (Dinosauria: Hadrosauridae) from the Late Cretaceous of Central Asia. *American Museum Novitates*, **3694**, 1–52.
- Prieto-Márquez, A., Erickson, G. M. and Ebersole, J. A. 2016. Anatomy and osteohistology of the basal hadrosaurid dinosaur *Eotrachodon* from the uppermost Santonian (Cretaceous) of southern Appalachia. *PeerJ*, **4**, e1872.
- R Core Team. 2021. R: a language and environment for statistical computing. Version 4.0.4. R Foundation for Statistical Computing. <https://www.R-project.org>
- Radley, J. D. 2006. A Wealden guide I: the Weald Sub-basin. *Geology Today*, **22**, 109–118.
- Ramírez-Velasco, A. A., Benammi, M., Prieto-Márquez, A., Ortega, J. A. and Hernández-Rivera, R. 2012. *Huehuenanautlus tiquichensis*, a new hadrosaurid dinosaur (Ornithischia: Ornithomimidae) from the Santonian (Late Cretaceous) of Michoacán, Mexico. *Canadian Journal of Earth Sciences*, **49**, 379–395.
- Rauhut, O. W. M., Remes, K., Fechner, R., Cladera, G. and Puerta, P. 2005. Discovery of a short-necked sauropod dinosaur from the Late Jurassic period of Patagonia. *Nature*, **435**, 670–672.
- Reisdorf, A. G. and Wuttke, M. 2012. Re-evaluating Moodie's opisthotonic-posture hypothesis in fossil vertebrates Part I: reptiles – the taphonomy of the bipedal dinosaurs *Compsognathus longipes* and *Juravenator starki* from the Solnhofen Archipelago (Jurassic, Germany). *Palaeobiodiversity and Palaeoenvironments*, **92**, 119–168.
- Reisz, R. 1972. Pelycosaurian reptiles from the middle Pennsylvanian of North America. *Bulletin of the Museum of Comparative Zoology at Harvard College*, **144**, 27–61.
- Revell, L. J. 2024. phytools 2.0: an updated R ecosystem for phylogenetic comparative methods (and other things). *PeerJ*, **12**, e16505.
- Rieppel, O. 1993. Patterns of ossification in the skeleton of *Alligator mississippiensis* Daudin (Reptilia, Crocodylia). *Zoological Journal of the Linnean Society*, **109**, 301–325.
- Rieppel, O. 1994. Studies on skeleton formation in reptiles. Patterns of ossification in the skeleton of *Lacerta agilis exigua* Eichwald (Reptilia, Squamata). *Journal of Herpetology*, **28**, 145–153.
- Romer, A. S. 1948. Relative growth in pelycosaurian reptiles. 45–55. In Du Toit, A. L. (ed.) *Robert Broom commemorative volume*. Royal Society of South Africa. Special Publication 45. 257 pp.
- Romer, A. S. 1956. *Osteology of the reptiles*. University of Chicago Press. 800 pp.



- Romer, A. S. and Price, L. J. 1940. Review of the Pelycosauria. *Geological Society of America, Special Paper*, **28**, 538.
- Ruiz-Omeñaca, J. I., Pereda Suberbiola, X. and Galton, P. M. 2007. *Callovosaurus leedsi*, the earliest dryosaurid dinosaur (Ornithischia: Euornithopoda) from the Middle Jurassic of England. 3–16. In Carpenter, K. (ed.) *Horns and beaks: Ceratopsian and ornithopod dinosaurs*. Indiana University Press. 384 pp.
- Saitta, E. T., Stockdale, M. T., Longrich, N. R., Bonhomme, V., Benton, M. J., Cuthill, I. C. and Makovicky, P. J. 2020. An effect size statistical framework for investigating sexual dimorphism in non-avian dinosaurs and other extinct taxa. *Biological Journal of the Linnean Society*, **131**, 231–273.
- Salgado, L. and Bonaparte, J. F. 1991. Un nuevo saurópodo Dicraosauridae, *Amargasaurus cazaui* gen. et sp. nov., de la Formación La Amarga, Neocomiano de la Provincia del Neuquén, Argentina. *Ameghiniana*, **28**, 333–346.
- Scheetz, R. A., Britt, B. B. and Higgerson, J. 2010. A large, tall-spined iguanodontid dinosaur from the Early Cretaceous (Early Albian) basal Cedar Mountain Formation of Utah. *Journal of Vertebrate Paleontology*, **30** (Suppl. 2), 158A. <https://doi.org/10.1080/02724634.2010.10411819>
- Seeley, H. G. 1888. On the classification of the fossil animals commonly named Dinosauria. *Proceedings of the Royal Society of London*, **43**, 165–171.
- Sereno, P. C. 1986. Phylogeny of the bird-hipped dinosaurs (Order Ornithischia). *National Geographic Research*, **2**, 234–256.
- Sereno, P. C., Beck, A. L., Dutheil, D. B., Gado, B., Larson, H. C. E., Lyon, G. H., Marcot, J. D., Rauhut, O. W. M., Sadleir, R. W., Sidor, C. A., Varricchio, D. D., Wilson, G. P. and Wilson, J. A. 1998. A long-snouted predatory dinosaur from Africa and the evolution of spinosaurids. *Science*, **282**, 1298–1302.
- Stewart, D. J. 1978. The sedimentology and palaeoenvironment of the Wealden Group of the Isle of Wight, southern England. PhD thesis. University of Portsmouth, 346 pp.
- Stovall, J. W. and Langstone, W. 1950. *Acrocanthosaurus atokensis*, a new genus and species of Lower Cretaceous Theropoda from Oklahoma. *American Midland Naturalist*, **43**, 696–728.
- Stromer, E. 1915. Ergebnisse der Forschungsreisen Prof. E. Stromers in den Wüsten Ägyptens. II. Wirbeltier-Reste der Baharije-Stufe (unterstes Cenoman). 3. Das Original des Theropoden *Spinosaurus aegyptiacus* nov. gen., nov. spec. *Abhandlungen der Königlich Bayerischen Akademie der Wissenschaften, Mathematisch-physikalische Klasse*, **28** (3), 1–32.
- Stutchbury, S. 1837. Description of a new species of the genus *Chameleon*. *Transactions of the Linnean Society*, **17**, 361–362.
- Sweetman, S. C. 2007. Aspects of the microvertebrate fauna of the Early Cretaceous (Barremian) Wessex Formation of the Isle of Wight, southern England. PhD thesis. University of Portsmouth, 316 pp.
- Sweetman, S. C. 2008. A spalacolestine spalacotheriid (Mammalia, Trechnotheria) from the Early Cretaceous (Barremian) of southern England and its bearing on spalacotheriid evolution. *Palaeontology*, **51**, 1367–1385.
- Sweetman, S. C. 2009. A new species of the plagiaulacoid multituberculate mammal *Eobaatar* from the Early Cretaceous of southern Britain. *Acta Palaeontologica Polonica*, **54**, 373–384.
- Sweetman, S. C. 2011. The Wealden of the Isle of Wight. 52–78. In Batten, D. J. (ed.) *English Wealden fossils*. The Palaeontological Association. Field Guide to Fossils 14. 780 pp.
- Sweetman, S. C. and Gardner, J. D. 2012. A new albanerpetontid amphibian from the Barremian (Early Cretaceous) Wessex Formation of the Isle of Wight, Southern England. *Acta Palaeontologica Polonica*, **58**, 295–324.
- Sweetman, S. C. and Insole, A. N. 2010. The plant debris beds of the Early Cretaceous (Barremian) Wessex Formation of the Isle of Wight, southern England: their genesis and palaeontological significance. *Palaeogeography, Palaeoclimatology, Palaeoecology*, **292**, 409–424.
- Taquet, P. 1976. *Géologie et paléontologie du gisement de Gadoufaoua (Aptien du Niger)*. *Cahiers de paléontologie*. Éditions du Centre National de la Recherche Scientifique, Paris, 191 pp.
- Taquet, P. and Russell, D. A. 1999. A massively constructed iguanodont from Gadoufaoua, Lower Cretaceous of Niger. *Annales de Paléontologie*, **85**, 85–96.
- Tompkins, J. L., LeBas, N. R., Witton, M. P., Martill, D. M. and Humphries, S. 2010. Positive allometry and the prehistory of sexual selection. *The American Naturalist*, **176**, 141–148.
- Tracy, C. R., Turner, J. S. and Huey, R. B. 1986. A biophysical analysis of possible thermoregulatory adaptations in sailed pelycosaurs. 195–206. In Hotton, N., Maclean, P. D., Roth, J. J. and Roth, E. C. (eds) *The ecology and biology of mammal-like reptiles*. Smithsonian Institution Press. 352 pp.
- Tsogtbaatar, K., Weishampel, D. B., Evans, D. C. and Watabe, M. 2019. A new hadrosauroid (Dinosauria: Ornithopoda) from the Late Cretaceous Baynshire Formation of the Gobi Desert (Mongolia). *PLoS One*, **14**, e0208480.
- Tsuihiji, T. 2004. The ligament system in the neck of *Rhea americana* and its implication for the bifurcated neural spines of sauropod dinosaurs. *Journal of Vertebrate Paleontology*, **24**, 165–172.
- van Devender, R. W. 1978. Growth ecology of a tropical lizard, *Basiliscus basiliscus*. *Ecology*, **59**, 1031–1038.
- Verdú, F. J., Godefroit, P., Royo-Torres, R., Cobos, A. and Alcalá, L. 2017. Individual variation in the postcranial skeleton of the Early Cretaceous *Iguanodon bernissartensis* (Dinosauria: Ornithopoda). *Cretaceous Research*, **74**, 65–86.
- Wagner, J. R. 2001. The hadrosaurian dinosaurs (Ornithischia: Hadrosauria) of Big Bend National Park, Brewster County, Texas, with implications for Late Cretaceous Paleozoogeography. MSc thesis. Texas Tech University, Austin, 417 pp.
- Wang, X., Pan, R., Butler, R. J. and Barrett, P. M. 2010. The postcranial skeleton of the iguanodontian ornithopod *Jinzhousaurus yangi* from the Lower Cretaceous Yixian Formation of western Liaoning, China. *Earth and Environmental Science Transactions of the Royal Society of Edinburgh*, **101**, 135–159.
- Weishampel, D. B., Jianui, C. M., Csiki, Z. and Norman, D. B. 2003. Osteology and phylogeny of *Zalmoxes* (n. g.), an unusual euornithopod dinosaur from the latest Cretaceous of Romania. *Journal of Systematic Palaeontology*, **1**, 65–123.
- Weishampel, D. B., Barrett, P. M., Coria, R. A., Le Loeuff, J., Xu, X., Zhao, X.-J., Sahni, A., Gomani, E. M. P. and Noto, C. R. 2004. Dinosaur distribution. 517–606. In Weishampel, D. B., Dodson, P. and Osmólska, H. (eds) *The Dinosauria*. University of California Press, Second edition. 861 pp.

- Welles, S. P. 1947. Vertebrates from the Upper Moenkopi Formation of northern Arizona. *University of California Publications in Geological Sciences*, **27** (7), 241–294.
- Wright, P. G. 1984. Why do elephants flap their ears? *South African Journal of Zoology*, **19**, 266–269.
- Wu, W. and Godefroit, P. 2012. Anatomy and relationships of *Bolong yixianensis*, an Early Cretaceous iguanodontoid dinosaur from Western Liaoning, China. 292–333. In Godefroit, P. (ed.) *Bernissart dinosaurs and Early Cretaceous terrestrial ecosystems*. Indiana University Press. 648 pp.
- Xu, X., Tan, Q., Gao, Y., Bao, Z., Yin, Z., Guo, B., Wang, J., Tan, L., Zhang, Y. and Xig, H. 2018. A large-sized basal ankylopollexian from East Asia, shedding light on early biogeographic history of Iguanodontia. *Science Bulletin*, **63**, 556–563.
- Zanno, L. E., Gates, T. A., Ayrahami, H. M., Tucker, R. T. and Makovicky, P. J. 2023. An early-diverging iguanodontian (Dinosauria: Rhabdodontomorpha) from the Late Cretaceous of North America. *PLoS One*, **18** (6), e0286042.